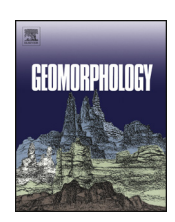
EI SEVIER

Contents lists available at ScienceDirect

Geomorphology

journal homepage: www.elsevier.com/locate/geomorph



Patterns and rates of riverbank erosion involving ice-rich permafrost (yedoma) in northern Alaska



Mikhail Kanevskiy ^{a,*}, Yuri Shur ^a, Jens Strauss ^b, Torre Jorgenson ^{a,c}, Daniel Fortier ^{a,d}, Eva Stephani ^a, Alexander Vasiliev ^{e,f}

- ^a Institute of Northern Engineering, University of Alaska Fairbanks, Fairbanks, USA
- ^b Alfred Wegener Institute Helmholtz Centre for Polar and Marine Research, Research Unit Potsdam, Potsdam, Germany
- ^c Alaska Ecoscience, Fairbanks, Alaska, USA
- ^d Geography Department, Université de Montréal, Montréal, Canada
- ^e Earth Cryosphere Institute, Moscow, Russia
- ^f Tyumen State Oil and Gas University, Tyumen, Russia

ARTICLE INFO

Article history: Received 2 May 2015 Received in revised form 21 October 2015 Accepted 26 October 2015 Available online 30 October 2015

Keywords: Thermal erosion Thermal denudation Ground ice Arctic Itkillik River Organic carbon

ABSTRACT

Yedoma, a suite of syngenetically frozen silty ice- and organic-rich deposits with large ice wedges that accumulated during the late Pleistocene, is vulnerable to thermal degradation and erosion because of the extremely high ice contents. This degradation can result in significant surface subsidence and retreat of coastal bluffs and riverbanks with large consequences to landscape evolution, infrastructure damage, and water quality. We used remote sensing and field observations to assess patterns and rates of riverbank erosion at a 35-m-high active yedoma bluff along the Itkillik River in northern Alaska. The total volumetric ground-ice content—including wedge, segregated, and pore ice—was estimated to be ~86%. The process of riverbank erosion and stabilization include three main stages typical of the areas with ice-rich permafrost: (1) thermal erosion combined with thermal denudation, (2) thermal denudation, and (3) slope stabilization.

Active riverbank erosion at the main study site started in July 1995, when the Itkillik River changed its channel. The total retreat of the riverbank during 1995–2010 within different segments of the bluff varied from 180 to 280 m; the average retreat rate for the most actively eroded part of the riverbank was almost 19 m/y. From August 2007 to August 2011, the total retreat varied from 10 to almost 100 m. The average retreat rate for the whole 680-m-long bluff was 11 m/y. For the most actively eroded central part of the bluff (150 m long) it was 20 m/y, ranging from 16 to 24 m/y. More than 180,000 m³ of ground ice and organic-rich frozen soil, or almost 70,000 metric tons (t) of soil solids including 880 t of organic carbon, were transported to the river from the retreating bank annually. This study reports the highest long-term rates of riverbank erosion ever observed in permafrost regions of Eurasia and North America.

© 2015 Elsevier B.V. All rights reserved.

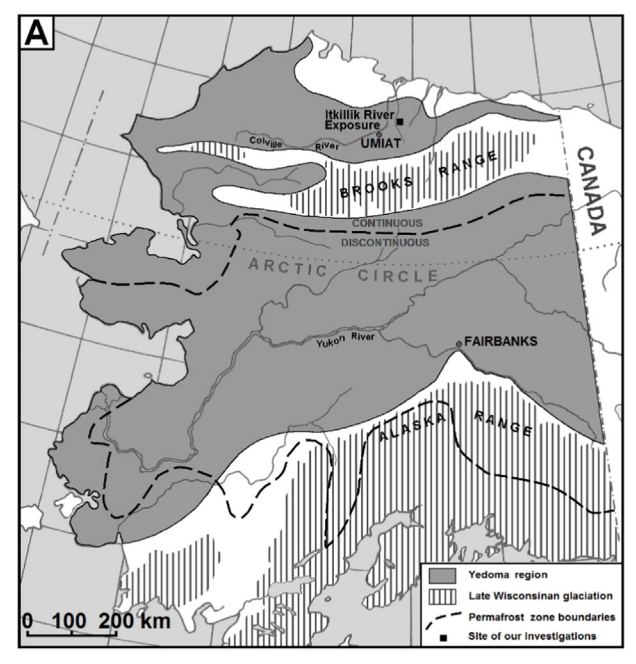
1. Introduction

Extremely ice-rich syngenetic permafrost, known as yedoma, is widespread in Alaska and Siberia. In this study, yedoma is used as a term for ice- and organic-rich syngenetically frozen silty sediments accumulated in the late Pleistocene (Kanevskiy et al., 2011; Schirrmeister et al., 2013). These deposits can be more than 40 m thick and they contain large ice wedges of up to 10 m wide, which usually vertically span the whole yedoma sequence. Yedoma in Siberia and

E-mail address: mkanevskiy@alaska.edu (M. Kanevskiy).

North America occupies ~420,000 km² (Strauss et al., 2013). It was formed in regions unglaciated during the late Pleistocene as a result of predominantly eolian, fluvial, and slope sedimentation (Tomirdiaro, 1980; Sher, 1997; Romanovskii et al., 2004; Kanevskiy et al., 2011; Schirrmeister et al., 2013; Murton et al., 2015). In the continuous permafrost zone of North America, yedoma is widespread in northern Alaska along the Arctic foothills (Carter, 1988; Kanevskiy et al., 2011; Jorgenson et al., 2014) and in the northern part of Seward Peninsula (Hopkins, 1963; Shur et al., 2012; Ulrich et al., 2014) (Fig. 1). In the discontinuous permafrost zone, yedoma has been observed at numerous sites of interior Alaska (Williams, 1962; Péwé, 1975; Hamilton et al., 1988; Shur et al., 2004; Bray et al., 2006; Kanevskiy et al., 2008, 2012, 2014; Jensen et al., 2013; Nossov et al., 2013) and Canada (Fraser and Burn, 1997; Kotler and Burn, 2000; Froese et al., 2009; Stephani et al., 2014).

^{*} Corresponding author at: 237 Duckering Bldg., P.O. Box 755910, Fairbanks, AK 99775-



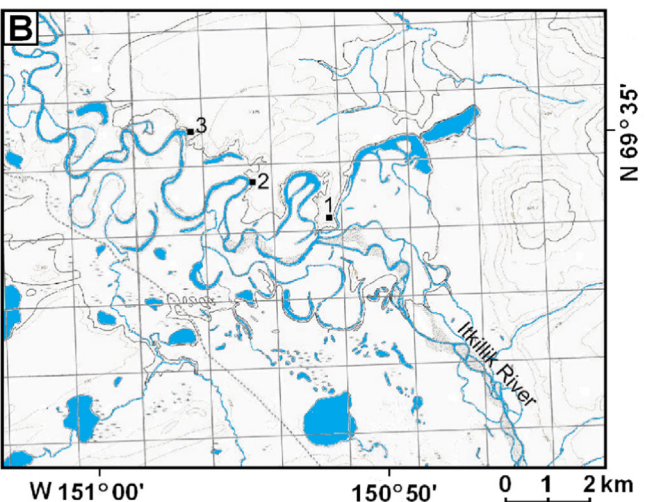


Fig. 1. (A) Location of the study sites. Boundaries of yedoma region (defined as area of potential yedoma occurrence) are shown after Kanevskiy et al. (2011); limits of late Wisconsinan glaciation are shown after Péwé (1975) and Hamilton (1994); and boundaries of permafrost zones are shown after Jorgenson et al. (2008). (B) Topographic map 1:63,360 (U.S. Geological Survey, 1971, based on aerial photographs taken in 1970) with location of study sites (marked with black squares). Study sites were described by Kanevskiy et al. (2011), Strauss et al. (2012b), and Murton et al. (2015) (site 1) and by Carter (1988) (sites 2 and 3).

Yedoma is vulnerable to thermokarst and erosion because of its high ice content and silty composition. Degradation of yedoma is mostly associated with formation of thermokarst lakes, which may result in surface subsidence of more than 20 m (Livingstone et al., 1958; Soloviev, 1962; Czudek and Demek, 1973; Ivanov, 1984; Carter, 1988; Brewer et al., 1993; Shur et al., 2012; Kanevskiy et al., 2014) with large consequences to landscape evolution, infrastructure damage, and water quality (Zaikanov and Kanevskiy, 1992a,b). Yedoma is also prone to river erosion, coastal erosion, formation of thermoerosional gullies, and surface ice-wedge degradation. Thermokarst and thermal erosion of ice-rich sediments creates serious hazards for the environment and infrastructure, which in some cases may require a costly relocation of villages. Coastal and riverbank erosion also releases large amounts of mineral and organic material that is transported to the Arctic Ocean (Reimnitz et al., 1988; Gordeev, 2006; Ping et al., 2011; Lantuit et al., 2013). Release of frozen organic matter upon yedoma thawing leads to changes in biogeochemical cycles and emission of greenhouse gases (Grosse et al., 2011; Strauss et al., 2012a; Schuur et al., 2015).

Processes and mechanisms of coastal, lakeshore, and riverbank erosion of the ice-rich sediments were described by Are (1968, 1980, 1985, 2012), Lawson (1983), Costard et al. (2003) Couture et al. (2008), Hoque and Pollard (2009), Jones et al. (2009, 2011), and Hinkel et al. (2012). Extensive data show that erosion rates in the Arctic are highly variable and strongly dependent on geomorphology and ground-ice content of permafrost (Miles, 1976; Are, 1980, 1985, 2012; Lawson, 1983; Rachold et al., 2000; Vasiliev et al., 2001; Shur et al., 2002; Vasiliev, 2003; Jorgenson and Brown, 2005; Lantuit et al., 2008, 2012, 2013; Jorgenson, 2011). While the average rate of coastal erosion for the entire Arctic coast is ~0.5 m/y, at numerous coastal segments the rates are much higher and vary with time (Lantuit et al., 2012, 2013). For example, Jones et al. (2009) found that for a 60-km segment of the Alaskan Beaufort Sea coast, characterized by 2- to 5-m-high bluffs with extremely ice-rich sediments, mean annual erosion rates reached 6.8 m/y (1955–1979), 8.7 m/y (1979–2002), and 13.6 m/y (2002– 2007). Solomon (2005) reported long-term retreat rates of up to 22.5 m/y at some sites in the Mackenzie Delta region of the Beaufort Sea, though such rates in this area were mostly related to wave activity rather than to high ice content of sediments.

Studies of riverbank and coastal erosion in the Russian Arctic revealed that the highest rates of erosion are typical mostly of yedoma bluffs, where they can reach more than 20 m/y (Are, 1985, 2012; Shur et al., 1984, 2002; Grigoriev, 2008; Günther et al., 2013). Long-term rates, however, are much smaller. At different sites of the Laptev Sea and East-Siberian Sea coasts they varied from 2 to 6 m/y (Are, 1985; Grigoriev, 2008), and for the entire coast with yedoma the rates of coastal erosion were estimated to be 2.1 m/y for the Laptev Sea and 1.8 m/y for the East-Siberian Sea (Grigoriev and Rachold, 2003; Grigoriev, 2008).

Most studies of erosion of yedoma bluffs are related to sea shores. Information on rates of riverbank erosion and the suite of successive processes that affect the thawing and collapse of yedoma deposits associated with river erosion is limited. Studies of erosion of yedoma riverbanks are available mainly for the Russian Arctic, where longterm erosion rates of such banks varied from 2 to 6 m/y (Shur et al., 1984, 2002; Are, 1985; Zaikanov and Kanevskiy, 1992a,b; Grigoriev, 2008), which are similar to the long-term rates of coastal erosion. In North America, most studies of riverbank erosion were not focused on the yedoma region. In Canada, long-term erosion rates of the banks of the southern Mackenzie River Delta based on aerial photographs varied from 1 to 11 m/y (Outhet, 1974). In northern Alaska, high erosion rates have been reported for the Sagavanirktok River (Brice, 1973; Scott, 1978) and for the Colville River (Walker and Arnborg, 1966; Walker, 1983; Walker et al., 1987; Walker and Jorgenson, 2011). The total retreat of the 8- to 10-m-high and 1.4-km-long bluff formed by ice-rich deposits with large ice wedges (similar to yedoma), located at the Colville River near the village of Nuiqsut, varied from 3 to 60 m from 1948 to 2004 (Walker and Jorgenson, 2011). Though the highest longterm rates of erosion at this site averaged for the whole observation period were slightly more than 1 m/y, in 1962 alone the retreat of a collapsing bank of about 10 m was reported (Walker et al., 1987). In interior Alaska, extremely fast riverbank erosion was described by Williams (1952) at the north bank of the Yukon River in the Yukon Flats area, where 10-m-deep niches could form in the ice-rich silt in two days, and the riverbank retreat could reach up to 60 m during one summer.

In this study, we describe and quantify the patterns and processes of degradation of the 35-m-high yedoma bluff along the Itkillik River in northern Alaska. The main objectives of this paper are to identify processes involved in degradation and stabilization of a riverbank formed by yedoma; measure short- and long-term rates of riverbank erosion and surface degradation; and assess amounts of mineral soil and organic carbon lost to erosion.

2. Study area

The study area is located in the middle reaches of the Itkillik River, which is a 350-km-long tributary of the Colville River—the major river of northern Alaska (Fig. 1A). Discharge measurements at the University of Alaska Fairbanks (UAF) lower Itkillik gauging site, located 16 km to the south of our main study site, were performed in 2012–2013 (Kane et al., 2014). In 2013, the lowest discharge (39 m³/s) was measured on July 12, and the highest (322 m³/s) on June 2, soon after the spring breakup. At that time, peak water level was more than 2 m higher than the lowest level measured in mid-July. Mean velocity during the summer 2013 varied from 1 to 2 m/s. Suspended sediment discharge at the Lower Itkillik gauging site had a single large peak during spring breakup of 2013 (more than 500 kg/s), while during the summer time the values were very low, with several short peaks of 50 to 90 kg/s registered in June and July (Kane et al., 2014).

The study area is located at the boundary of the Beaufort Coastal Plain and the Brooks Range foothills and characterized by extremely cold climate. Mean annual air temperature (MAAT) in Umiat (54 km to the southwest of our main study site) averaged for the period from 1987 to 1992 was $-12.7\,^{\circ}\mathrm{C}$ (Zhang et al., 1996). Based on the data of UAF meteorological station (DUS2, Anaktuvuk River), located 17 km to the southwest of our main study site, MAAT equal to $-10.2\,^{\circ}\mathrm{C}$ was found for the period 2009–2013 (Kane et al., 2014). Warm season precipitation at the same station varied from 86.5 to 145.2 mm (112 mm average), and snow water equivalent varied from 82 to 107 mm. The study area belongs to the continuous permafrost zone. Permafrost thickness in this part of northern Alaska varies from 200 to 300 m, and mean annual permafrost temperature at the depth of zero annual amplitude varies from $-5\,$ to $-7\,^{\circ}\mathrm{C}$ (Jorgenson et al., 2008).

Our field study was mainly conducted on the 35-m-high and 680-m-long vertical yedoma bluff (site 1 in Fig. 1B, 69°34′ N, 150°52′ W) with large syngenetic ice wedges (Fig. 2, Figs. S1 to S9 in Supplementary materials) from August 2006 to May 2012 during the four field trips (Kanevskiy et al., 2011; Strauss et al., 2012b). Prior to our study, Carter (1988) described two smaller exposures (sites 2 and 3 in Fig. 1B) located 2 and 3.5 km to the northwest from site 1. All three sites belong to the same large remnant of the flat yedoma plain elevated ~35 m above the current Itkillik River water level and 90 masl (Fig. 1B). Carter (1988) interpreted the permafrost of these sites as syngenetic and suggested that it may be common for the area of lower foothills, which he defined as the northern Alaska silt belt formed by eolian



Fig. 2. Aerial view of 35-m-high exposure of the Itkillik yedoma site 1, August 2011. Numbers represent stages of riverbank degradation and stabilization (Table 2). Note increased turbidity of the river from sediment input.

sediments. Our interpretation of aerial photographs and satellite images supports his suggestion (Kanevskiy et al., 2011).

3. Methods

3.1. Soil characterization and evaluation of ground ice volume

We described the exposed bluff and drilled boreholes with a SIPRE corer (7.5 cm in diameter) at various elevations at accessible parts of the exposure. A GPS (eTrex Vista C) and an auto-level were used to survey the positions of boreholes and the edge of the bluff, and their respective elevations above the Itkillik River water level. Cryostructures (patterns formed by ice inclusions in the frozen soil) were described using a classification (Kanevskiy et al., 2011, 2013a) adapted from several Russian and North American classifications. More than 150 samples of frozen soil were taken in 2007 and 2011 to estimate gravimetric and volumetric moisture contents (GMC and VMC), bulk density (BD), and dry density (DD). To determine these values, initial weights of samples of frozen soil and their weights after oven-drying (90 °C, 72 h) were measured; volumes of frozen samples were calculated by measuring the length and diameter of the cores. The values are presented as mean \pm standard deviation. Twenty soil samples obtained in 2007 were analyzed for total C and N (Kanevskiy et al., 2011).

Field and laboratory analyses for evaluation of the total organic carbon (TOC) content and BD were also conducted on 43 samples transported frozen to the laboratory in May 2012. For BD calculation, sample volume measurements were performed in the field by determining the water volume displaced by the sealed frozen sample submersed in a glass beaker filled with water. The BD was calculated using dry weight determined after freeze-drying in the laboratory (Sublimator 3-4-5, ZIRBUS Technology). For laboratory analysis (Strauss et al., 2012b), the samples were homogenized using a planetary mill. Soil samples were processed twice using a TOC analyzer (Elementar Vario Max C) with automatic carbonate removal. In each series of measurements, a blank capsule was used for background detection and standards were measured after every 15 samples to ensure correct analytical values with a device-specific accuracy of \pm <1 wt.%. To calculate the organic carbon density, the BD measurements were combined with TOC values and wedge-ice volume. Total organic carbon density (TOCD, kg/m³) was calculated according to the equation (Strauss et al., 2013):

$$TOCD = BD \left(10^3 kg/m^3\right) \times \frac{TOC}{100} \times 1000. \tag{1} \label{eq:toch_prop}$$

In this carbon density calculation, we did not include the wedge-ice volume. For an overall bluff carbon density as needed for carbon flux calculation, we subtracted the wedge-ice volume separately. Additionally, TOC values obtained earlier from 20 samples (Kanevskiy et al., 2011) were included in the calculations. The TOC content of wedge ice was neglected as it is not significant in comparison with yedoma soils (Fritz et al., 2015).

Overall wedge-ice volume in the exposure was estimated through photogrammetric analysis. Panoramic photographs of the exposure taken in 2006, 2007, 2011, and 2012 were transformed into binary (black and white) images. The area occupied by wedge ice was measured using ImageJ software (Ferreira and Rasband, 2012). The total volumetric ground ice content of the Itkillik yedoma was estimated by the following equation (Grechishchev and Shur, 1990; Kanevskiy et al., 2013b):

$$TVIC = WIV + VICS \times (1 - WIV), \tag{2}$$

where WIV — wedge-ice volume, unit fraction; VICS — volumetric ice content of soils between ice wedges (includes pore and segregated ice), unit fraction.

3.2. Evaluation of rates of erosion

The rate of erosion was evaluated by two methods. For the evaluation of the short-term erosion rate, the GPS was used to locate position of the riverbank and the top of the retreating bluff in August 2007, August 2011, and May 2012. For better accuracy, waypoints during GPS surveying (with differential Wide Area Augmentation System enabled) were averaged over time with 50–100 readings (estimated accuracy ± 3 m). For more accurate measurements of riverbank erosion, several benchmarks were installed on the main yedoma surface in August 2007 to a distance of 40 m from the bluff, but all benchmarks were lost to erosion by August 2011, which shows that the average rate of erosion was > 10 m/y. Longterm erosion rate was evaluated based on analysis of topographic maps, aerial photographs, and satellite images available from Google Earth, the Geographic Information Network of Alaska (GINA) of the University of Alaska http://www.gina.alaska.edu/), and the U.S. Geological Survey (http://earthexplorer.usgs.gov/).

3.3. Estimation of volume of eroded soil and organic carbon

The data on mass and volumes of ice, mineral, and organic components of the yedoma and data on the retreat rates of the bluff were used to estimate the amount of material lost annually from the eroding bluff. For this estimate, we divided the exposure into several segments with different modes of riverbank degradation observed from 2007 to 2011. For each segment, the total volume of frozen soils transported annually to the river $(V, m^3/y)$ from the retreating bank was estimated:

$$V = L \times H \times R, \tag{3}$$

where L — length of segment, m (average between 2007 and 2011); H — average height of the bluff adjusted for calculations (equal to average height of the actively eroding parts of the bluff; for the segments of completely exposed vertical bluff, H is equal to the total height of the bluff above the river level), m; R — average retreat rate in 2007 to 2011, m/y.

The WIV, DD, and TOCD values were used to estimate a dry weight of solids, including mineral and organic components (DWS), and organic carbon (DWOC) transported to the river:

$$DWS = DD \times V \times (1 - WIV) \tag{4}$$

$$DWOC = TOCD \times V \times (1 - WIV). \tag{5}$$

4. Results and discussion

4.1. Yedoma soils and ground ice

Yedoma deposits consist of the mineral solids, organic remnants of plants and animals, pore and segregated ice, and massive wedge ice between soil columns. At site 1 (site location is shown in Fig. 1), mineral solids of presumably eolian origin were dominated by coarse silt (Murton et al., 2015). Cryostratigraphy of permafrost at this site was previously described by Kanevskiy et al. (2011). We defined seven cryostratigraphic units (described from the top), including: (1) active layer at 0 to 0.6 m; (2) contemporary intermediate layer (ice-rich silt) at 0.6 to 1.5 m (Fig. S6); (3) silt with relatively thin ice wedges at 1.5 to 14 m; (4) silt with thick ice wedges at 14 to 27 m; (5) buried peat layer at 27 to 29 m; (6) buried intermediate layer at 29 to 31 m; and (7) silt with small buried ice wedges at 31 to >33 m. Drilling at the base of the bluff, performed in August 2011, encountered alluvial gravel at depth of 1.5 m below the river level. Gravimetric moisture content of soils between ice wedges varied from 148 wt.% in the intermediate layer (average for unit 2) to 59 wt.% in yedoma (average for units 3 and 4); average value for the entire section was 70 \pm 41 wt.%. Average

volumetric moisture content of soils between ice wedges for the entire section was 65 ± 10 vol.%, and average BD and DD were 1.58 ± 0.19 and 0.97 ± 0.27 g/cm³, respectively.

Kanevskiy et al. (2011) defined four generations of ice wedges forming different polygonal networks. Small Holocene ice wedges occurred within the intermediate layer (unit 2). These epigenetic wedges, triangular in shape, were up to 2 m wide (by width we mean the *true* width of ice wedges, measured in cross sections perpendicular to the ice-wedge direction) and up to 4 m tall; usually they penetrated into the late Pleistocene syngenetic ice wedges of unit 3 (Fig. S6). The latter were relatively wide at the top (up to 5 m), and their width decreased gradually with depth. The spacing between ice wedges varied from 7 to 10 m. Ice wedges in unit 4 were up to 10 m wide and their width remained fairly constant with depth. Most of them persisted below the Itkillik River water level. Ice wedges in unit 7, located at the bottom of the exposure beneath the peat layer, were <0.7 m in width and 2.5 to 3 m in height. The spacing between ice wedges varied from 3 to 8 m.

Wedge-ice volume varied from 40 to 52 vol.% in cryostratigraphic units 2 to 3 (45 vol.% average) and from 71 to 81 vol.% in units 4 to 7 (78 vol.% average). Evaluations were performed for the central section of the exposure (AB in Fig. 3). Wedge-ice volume for the entire exposed bluff varied from 52 to 66 vol.% (61 vol.% average) (Table 1). The accuracy of measurements of wedge-ice volume with ImageJ was relatively high as indicated by the similar estimates derived from photographs taken on 13 and 19 August 2011 from different vantage points (Table 1; Fig. 3).

Variations in wedge-ice volume can be explained by different orientations of ice wedges at the time of their exposure. When the majority of exposed wedges were more or less perpendicular to the exposure, the area occupied by wedge ice was the smallest (for example, such orientation of wedges prevailed in units 4 to 7 on 14 May 2012 and in units 2 to 3 on 3 August 2006; compare Fig. 3 and Table 1). The lowest wedge-ice volume for the entire bluff of 52 vol.% was estimated for 3 August 2006, compared to 59–66 vol.% for the other dates. We attributed this difference to the relatively small area of the lower part of the bluff exposed at that time, considering that the highest volume of wedge ice was typical of units 4 to 7.

The total volumetric content of ground ice (TVIC) of the Itkillik yedoma was estimated to be 86 vol.% when combining proportional volumes of wedge ice (61 vol.%) and ice content of soils between ice wedges (65 vol.%) (Eq. (2)).

Total organic content (TOC) ranged from 0.1 to 31.4 wt.% with a mean value of 1.8 wt.%, and median TOC of 0.8 wt.%. The mean TOC density was 12.3 kg/m 3 (median 8.4 kg/m 3) in the soils between the ice wedges (Eq. (1)). When compensating for the ice-wedge volume of 61%, the mean carbon density was 4.8 kg/m 3 (median 3.3 kg/m 3).

4.2. Processes and stages of riverbank erosion

Riverbank erosion in the study area occurs mainly in forms of thermal erosion and thermal denudation, which is typical of ice-rich permafrost areas. Thermal erosion is a process of combined thermal and mechanical action of moving water that results in simultaneous thawing of frozen ice-bearing deposits and its removal by water (van Everdingen, 1998; Shur and Osterkamp, 2007). Removal of thawed deposits constantly exposes the frozen face of the bluff. Thermal erosion is the most effective process of permafrost degradation. Rates of thermal erosion are about two orders of magnitude greater than those of thermokarst, related to thawing of permafrost by heat conduction with accumulation of the thawed material over permafrost (Shur, 1988). Moreover, thermal erosion is about an order of magnitude more effective than permafrost thawing in contact with standing water (Shur, 1988). For example, on Bylot Island (Canadian Arctic Archipelago), thermal erosion has led to fast degradation of an ice-wedge

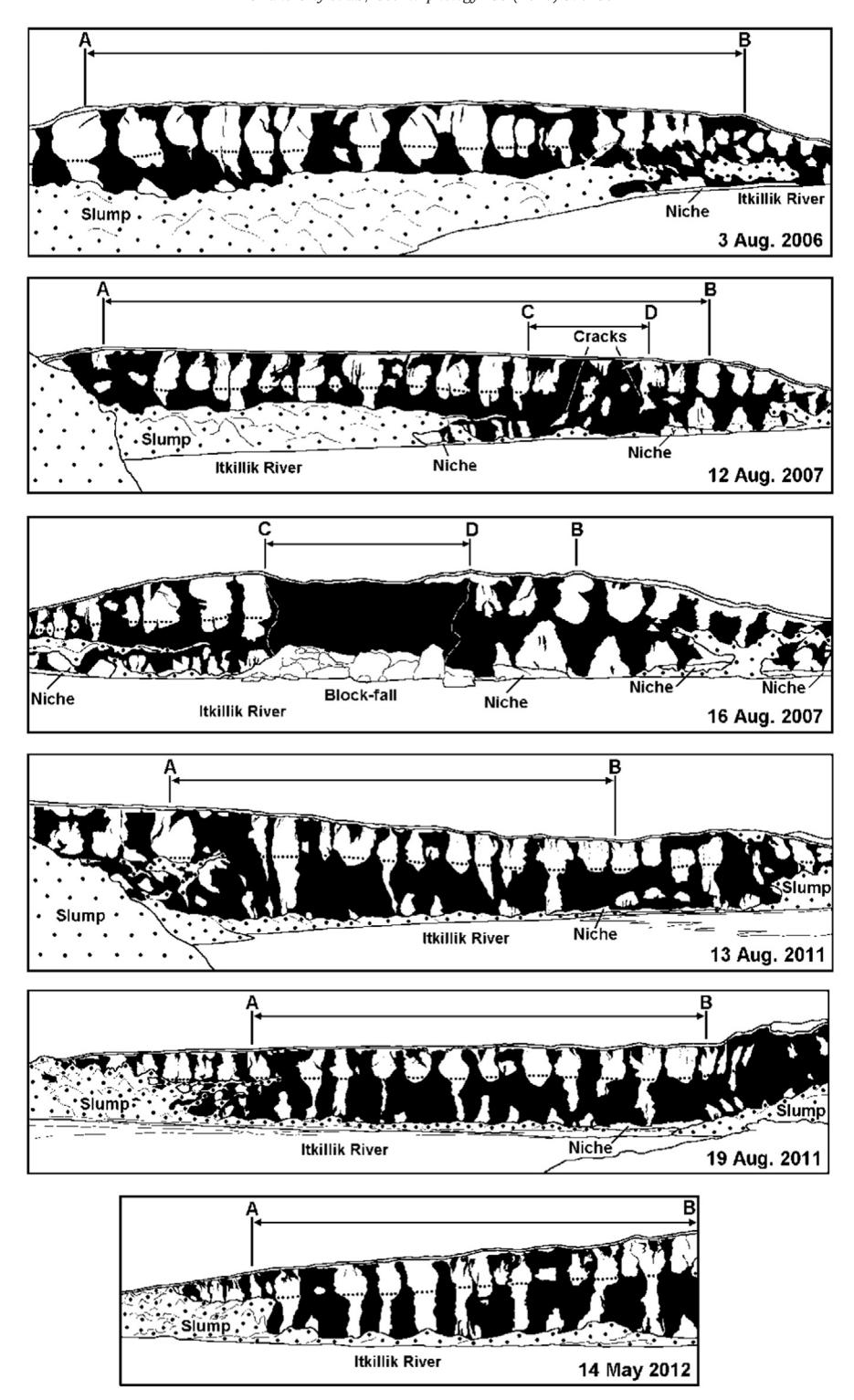


Fig. 3. Wedge ice (black) in the exposed bluff in 2006 to 2012, site 1. AB — a 240-m-long section of the central part of the bluff that was used for estimations of wedge-ice volume (Table 1); CD — an area of block fall on 16 August 2007. Dotted line shows the boundary between units 3 and 4.

Table 1Relative volume (%) of visible wedge ice in sections AB of the bluff.

Date	Units 2 to 3	Units 4 to 7	Entire bluff
3 August 2006	39.6	78.3	52.3
12 August 2007	51.9	78.4	62.4
13 August 2011	45.7	80.3	65.9
19 August 2011	43.8	81.3	66.3
14 May 2012	43.0	70.7	59.3
Average \pm standard deviation	44.8 ± 4.5	77.8 ± 4.2	61.2 ± 5.8

network with rapid formation of new drainage systems (Fortier et al., 2007; Godin and Fortier, 2012).

Thermal denudation is a process of thawing of frozen soils on the exposed bluff surface caused by solar radiation and convective heat exchange between the cold surface and the atmosphere, and subsequent removal of thawed soils from the bluff by gravity (Are, 1968, 1980, 1988; Shur and Osterkamp, 2007). The removal of thawed soil occurs in forms of flow and microfalls of thin layers of thawing soil from the exposed face of the bluff. Thermal denudation is triggered by thermal

Table 2Main stages and processes of the riverbank erosion and stabilization^a.

Stage	Substage
Stage 1: Thermal erosion combined with thermal denudation	1a: Formation of thermoerosional niches at the base of the riverbank; thermal denudation of the exposed face 1b: Development of subvertical cracks above the niche/block fall; thermal denudation of the exposed face 1c: Thawing and disintegration of the collapsed blocks of ground ice and frozen soil in the river and at the base of the bluff;
	thermal denudation of the exposed face 2a: Thermal denudation of the exposed face; formation of the sediment bar protecting the vertical bluff from river erosion, removal of thawed material during flooding events by mechanical erosion
Stage 2: Thermal denudation	2b: Thermal denudation of the exposed face; decrease in the height of the exposed vertical bluff; accumulation of thawed material and grading of the slope; gully erosion, sheet erosion and mudflows; formation of thermokarst mounds (baydzherakhs); early plant establishment at the base of the slope
Stage 3: Slope stabilization	3a (Early): Lack of headwall as a result of coverage of the exposed bluff with thawed and displaced sediments; gully erosion, sheet erosion, and mudflows at some parts of the slope; vegetation growth 3b (Late): Complete vegetation cover on the stabilized slope; decrease in the active layer depth; permafrost aggradation

^a Notes: Thermal erosion and mechanical erosion refer to riverbank erosion only. Gully erosion may include both thermal and mechanical mechanisms. Sheet erosion is mechanical (downslope removal of thin layers of unfrozen soil by sheetflow).

erosion and starts as soon as the ice-rich permafrost at the bluff is exposed. Thermal denudation continues for years (and even decades on high vertical bluffs with ice-rich soils and massive ice bodies) after the termination of thermal erosion (Are, 1980, 2012; Shur et al., 2002).

Based on the relative importance of thermal erosion and thermal denudation, three main stages of the riverbank evolution were defined for the study area (Tables 2, S1 in Supplementary materials; Figs. 2, 4).

4.2.1. Stage 1: thermal erosion combined with thermal denudation

Thermal erosion of riverbanks begins with the bank undercutting and formation of thermoerosional niches at the base of the riverbank (substage 1a). Growth of thermoerosional niches eventually leads to free fall of blocks of ice and frozen ground (substage 1b). It occurs when stress on frozen soil and ice from increasing weight of frozen soil above niches overcomes the long-term strength of frozen soil or ice. Fall usually occurs along ice wedges, which form planes of weakness because the long-term shear strength of ice is smaller than that of frozen ground; it often results in the collapse of entire polygonal blocks (Leffingwell, 1915, 1919; Are, 1968, 1988; Hoque and Pollard, 2009; Fortier and Allard, 2004). Block falls are preceded by development of subvertical cracks above the thermoerosional niches, at several to dozens of meters behind the bluff. Our observations show that the time between the crack formation and collapse of the bluff varies from several hours to several months. Ground ice and frozen soil of fallen blocks thaw and disintegrate quickly in the river and much slower if they accumulate at the base of the bluff (substage 1c). Depending on the volume of collapsed material, duration of substage 1c varies from several days to several weeks.

Thermal erosion during *substages 1a, 1b,* and *1c* is accompanied by thermal denudation of the exposed bluff above niches. Thus, the degradation of the bluff during *stage 1* is governed by thermal erosion and thermal denudation simultaneously. Thermal denudation at *stage 1* reduces the total rate of erosion because it reduces the size of blocks of frozen soil above niches and therefore increases the duration of time periods between block-fall events. During the development of niches, the part of the bluff above niches retreats with a rate entirely defined by thermal denudation.

Deep thermoerosional niches (*substage 1a*) have been observed during every visit to site 1. The niches were incised in the base of the bank for more than 10 m, and their height at openings varied from 1 to 3 m (Fig. 5A). In August 2006, the niches developed only at the southern part of exposure, within the south-facing slope of the yedoma remnant up to its boundary with the floodplain (Fig. 3), and their total lateral extent reached ~250 m. At that time, the foot of the northern part of the exposure was relatively stable, and the exposed vertical bluff (*active bluff* in Fig. 4A) of up to 15 m height was located about 80 m from the river and retreated solely because of thermal denudation. Only a small portion of this relatively gentle slope was affected by thermal erosion (Fig. 3). During summer 2007, the development of niches continued northward, and their total length in August 2007 exceeded 300 m

(Figs. 3, 4). By August 2011, the total length of active niches decreased to <65 m. Along a significant part of the riverbank, inactive niches at that time were protected from further development by a very low and narrow (<15 m) bar. However, this bar could be easily eroded by the river creating a high probability that new niches could form the following spring within another 100 to 150 m of the bank (Figs. 2, 3, 4).

On 15 August 2007, we observed several wide and deep semicircular cracks formed on the yedoma surface at distances up to 15 m from the edge of the bluff (*substage 1b*). The visible depth of cracks exceeded 10 m, and their width reached 1.5 m (Fig. 5B). A vertical displacement of up to 0.5 m along the cracks was also observed. More likely, formation of these cracks started much earlier: sub-vertical cracks were already visible on the exposed face of the bluff on 12 August 2007 (Fig. 3), though at that time we could not find any manifestation of cracks on the ground surface. On 16 August at 5 a.m., crackling noises were heard for several minutes and suddenly a very large portion of the bluff collapsed down with a strong sound and created a large splash in the river (Figs. 5C, 6). The block fall affected the upper 20-m portion of the bluff. The lower part of the bluff had probably experienced a similar block fall prior to our arrival to the site, as evidenced by a sharp negative angle of the lower part of the bluff.

The block fall occurred along the cracks formed in ice wedges subparallel to the bluff, and the wall exposed after the collapse was entirely composed of wedge ice (Fig. 3, 16 August 2007). The length of the ice wall measured on top of the bluff was >65 m. The area on the main yedoma surface involved in the block fall was ~800 m² (Fig. 4), and its volume was ~15,000 m³. Some of the collapsed blocks were up to 10–15 m across (Figs. 3, 6). Fragments of massive ice and frozen soil, many of them up to 2 m across, were scattered within a distance of ~300 m from the bluff. Most of the fragments submerged in water thawed and completely disintegrated within a few hours ($substage\ 1c$), while at the base of the bluff and on the opposite bank this process was much slower. When we left the site on 18 August 2007, most of the fragments on the banks were still visible.

No cracks on the main surface of yedoma were found in August 2011, but in May 2012 we observed large cracks near the bluff (Figs. 4A, S8), most of them developed along ice wedges. The total length of cracks was almost 100 m, their width varied from 0.5 to 4 m, and their visible depth from 5 to 13 m. These cracks were also detected on photographs taken on 23 June 2012 (A. Breen, UAF, pers. com., 2012) (Fig. S9). Presumably, the block fall occurred in late June or July, because no cracks or recently collapsed fragments were observed on 12 August 2012 by B. Abbott (UAF, pers. com., 2012).

From 2007 to 2011 erosion of a significant part of the Itkillik bluff remained very active (Fig. 4A, sections 4 and 5 in Fig. 4B), while other segments of the actively eroded riverbank evolved into *substages 2a* (section 3), *2b* (section 6), and even *3a* (section 7). In the latter case, such a rapid transformation was possible because of the low height (about 6 m) of the eroded bluff (Fig. 4B).

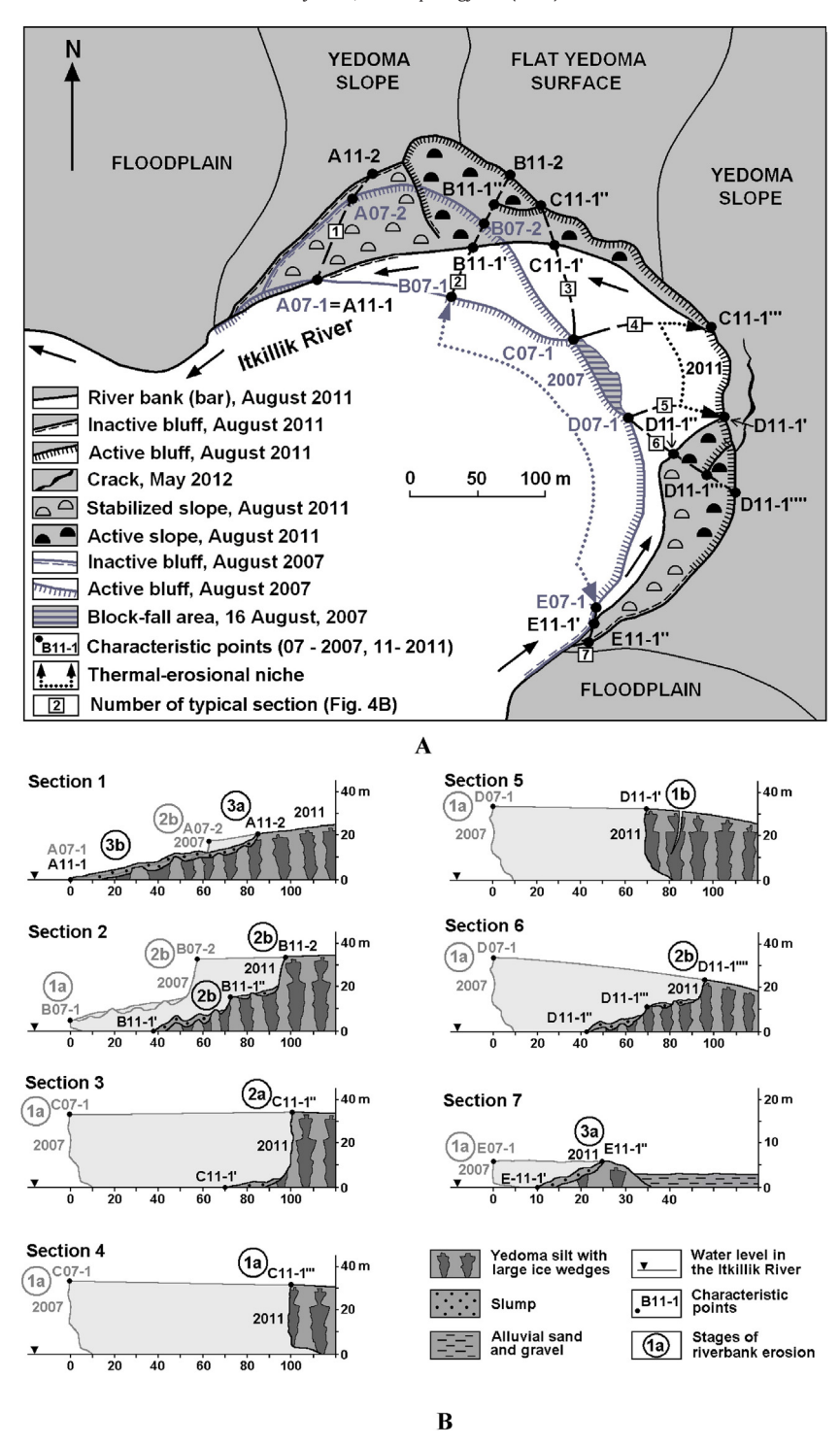


Fig. 4. (A) Geomorphic map of the Itkillik River exposure (site 1) showing positions of the bluff in August 2007 (gray) and August 2011 (black) with characteristic points. (B) Typical sections of the retreating bluff and stages of riverbank erosion and stabilization in 2007 and 2011. The stages of riverbank erosion and stabilization (black and gray numbers with letters in circles) are defined in Table 2.

4.2.2. Stage 2: thermal denudation

This stage begins when the rate of accumulation of thawed and displaced sediments at the base of the exposed bluff becomes equal to or exceeds the rate of river erosion. In this case, the contact of running water with the bluff occurs mainly during the spring runoff, and its role is limited by removal of products of thermal denudation accumulated at the base of the bluff during the previous year. The retreat of the bluff is entirely defined by thermal denudation, but its products are removed by water so that the bluff can remain vertical (*substage 2a*).

For most of the warm season, the low and narrow bar, covered by the products of debris from the retreating bluff (Fig. 5D) separates the bluff from the river. Between 2007 and 2011, the transformation from *stage 1* to *substage 2a* occurred at the central part of the bluff (section 3 in Fig. 4). *Substage 2a* can continue for several years; its duration is defined by the balance between accumulation and erosion of soil at the base of the bluff. Because of extremely high ice content of yedoma, soil accumulation at the base of the bluff is low, so it can be easily removed by running water. An increase in erosion activity results in formation of

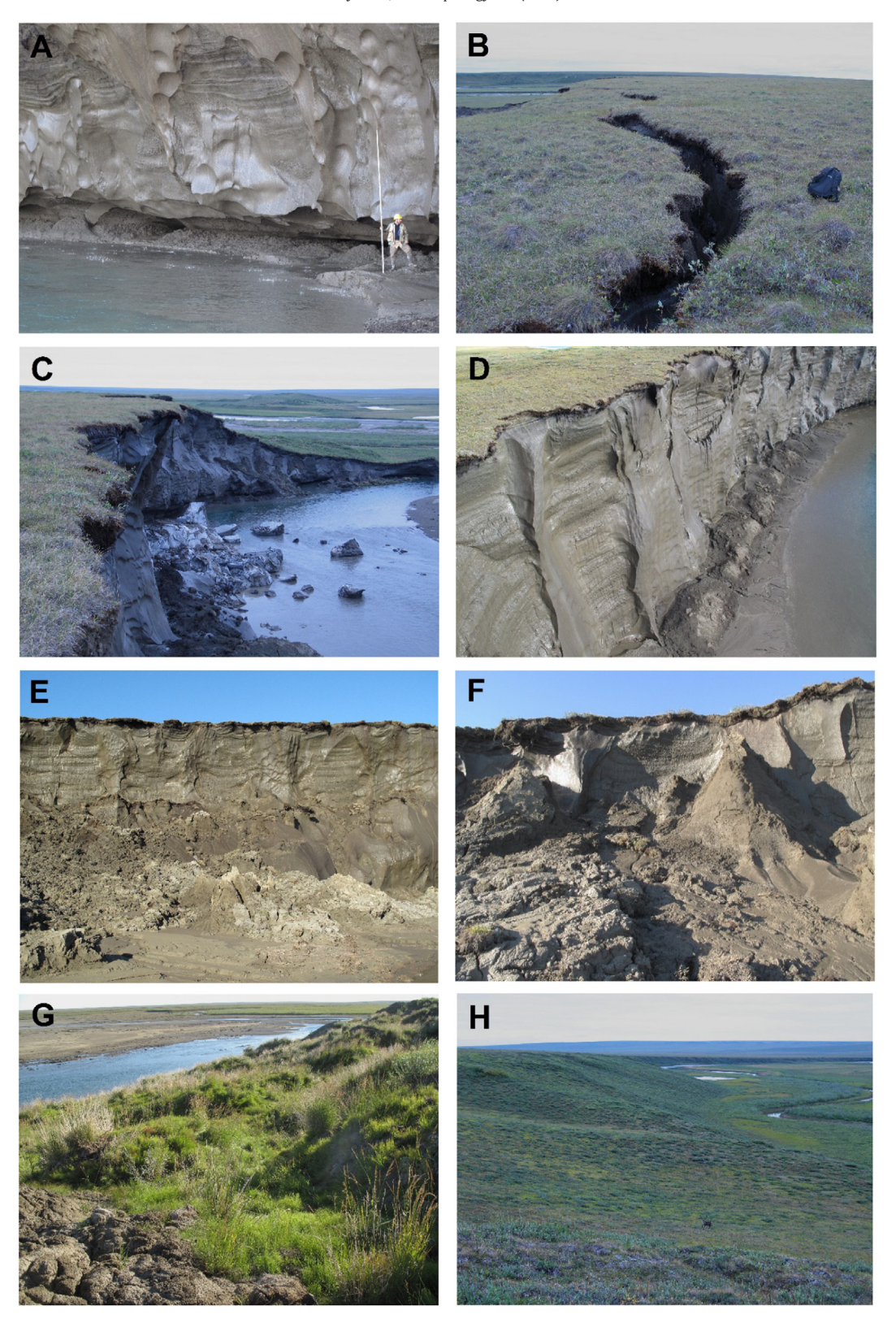


Fig. 5. Stages and processes of the riverbank erosion, site 1. (A) *Substage 1a*, thermoerosional niche at the base of the bluff, thermal denudation, August 2011. (B) *Substage 1b*, large cracks on top of the bluff, 15 August 2007 (0.5-m-tall backpack is for scale). (C) *Substage 1c*, block fall, 16 August 2007 (height of the bluff is up to 35 m). (D) *Substage 2a*, thermal denudation, debris fall, and accumulation (height of the bluff is up to 35 m). (E) *Substage 2b*, thermal denudation, mudflow, sheet flow, and rill erosion (height of the vertical part of the bluff is up to 30 m). (F) *Substage 2b*, thermal denudation, mudflow, early stage of baydzherakh formation (height of the vertical part of the bluff is up to 12 m). (G) *Substage 3a*, early slope stabilization, differential thaw settlement, partially vegetated baydzherakhs up to 3 m high. (H) *Substage 3b*, complete slope stabilization, south-facing slope of the yedoma remnant (height of the slope is ~30 m).

thermoerosional niches and reversion to *stage 1*. A decrease in activity of the river erosion terminates *substage 2a* and triggers its transformation to *substage 2b*.

Continuing accumulation of debris at the base of the bluff protects the underlying permafrost from thawing. The bluff, previously subvertical for its entire height, becomes relatively gentle in its lower part, while its upper part, affected by thermal denudation, remains subvertical (*substage 2b*). The height of this vertical part continually decreases with time. This process lasts from years to decades depending on ice content, bluff height, relief behind the bluff, and climate (Shur et al., 2002).

Between 2007 and 2011, the transformation from *stage 1* to *substage 2b* occurred in the southern part of the studied bluff (section 6 in Fig. 4). Evolution of the riverbank during *substage 2b* is illustrated by section 2 (compare profiles B07-1–B07-2 and B11-1″–B11-2 in Fig. 4B). The average rate of thermal denudation around this section was ~11 m/y, and the height of vertical bluff decreased from ~20 m in 2007 to <15 m in 2011. Reactivation of thermal erosion at the base of the gentle partially stabilized slope (observed in 2007, see point B07-1 in Fig. 4B, *substage 1a*), completely terminated by 2011 when no exposed permafrost could be observed within the lower part of the riverbank (point B11-1′ in Fig. 4B). This new cycle of riverbank erosion resulted in formation of the secondary thermo-denudational bluff up to 7 m high visible at the middle part of the slope (point B11-1″ in Fig. 4B, *substage 2b*).

During *substage 2b*, thermal denudation of the upper (exposed) part of the bluff creates accumulation of melt water at the bottom of the vertical bluff, which triggers slumping, mudflow, rill and sheet erosion, and formation of thermoerosional gullies within the lower slope (Fig. 5E, F), which is labeled *active slope* in Fig. 4A. Additionally, thawing of permafrost beneath a thin layer of thawed and displaced sediments in the lower slope results in differential thaw settlement, which contributes to formation of conical thermokarst mounds (baydzherakhs) (Shur and Vasiliev, 1978; French, 2007) surrounded by degrading ice wedges (Fig. 5F).

All these processes lead to flattening of the lower part of the slope, consequent termination of thermal denudation, and slope stabilization. During this substage, vegetation growth starts at the base of the slope, while its upper part still experiences thermokarst and thermal denudation.

4.2.3. Stage 3: slope stabilization

Decrease in height of the exposed yedoma bluff to <4.5 m leads to a fast decrease in retreat rates and termination of thermal denudation within several years (Shur et al., 2002). As a result of this process, the vertical part of the bluff transforms into a relatively gentle slope. Accumulation of soil on the reduced slope finally leads to complete coverage of the slope with thawed and displaced soil (*substage 3a*). A lack of an

exposed headwall results in decreased water and sediment input and in drainage of sediments.

During this substage, thawing of permafrost still continues in the upper part of the slope beneath a thin layer of thawed and displaced sediments, but the rate of thaw subsidence becomes lower with a thickening of this layer. Numerous baydzherakhs, which have formed as a result of gully erosion and differential thaw settlement during *substages* 2b and 3a, have partially degraded because of mechanical erosion and gravitational processes; but the rapid growth of vegetation leads to a decrease in active layer thickness and slope stabilization (Fig. 5G, *stabilized slope* in Fig. 4A).

Transformation from *stage 2* to *substage 3a* usually takes from several years to several decades, depending on the initial height of the exposed bluff. For example, the 3-m-high vertical bluff completely disappeared between 2007 and 2011, and no frozen material was exposed at this part of the slope by August 2011 (section 1 in Fig. 4). Under certain conditions, the entire cycle from *substage 1a* to *substage 3a* can be completed in several years. This happened in the southern part of the exposure, where the 5- to 8-m-high vertical bank (section 7 in Fig. 4B) was actively degrading in 2007 (*stage 1* with deep thermoerosional niches), but by August 2011 the bank transformed into a gentle slope completely covered by thawed and reworked sediments.

Slope stabilization completes with termination of thermokarst caused by a decrease in active layer depth triggered by vegetation growth, which leads to formation of the intermediate layer (Shur, 1988; Shur and Osterkamp, 2007; Kanevskiy et al., 2011, 2013a) and permafrost aggradation. The slope becomes practically stable when the vegetation covers its entire extension (*substage 3b*). Baydzherakhs can still be visible for many decades (Shur, 1988), but their height gradually decreases from soil slumping and creep, and eventually they have little to no surface expression (Fig. 5H). Such gently graded slopes can remain stable until they are reactivated by a new cycle of riverbank erosion.

4.3. Short- and long-term erosion rates

4.3.1. Rates of riverbank retreat at site 1

From August 2007 to August 2011, riverbank retreat at site 1 varied from <10 to almost 100 m across different parts of the exposure (Fig. 4A). The total lost area of the yedoma surface on top of the bluff for this period was 30,880 m². Over the four-year period, the average retreat rate for the entire 680-m-long bluff was 11.4 m/y. For the most



Fig. 6. Block fall of the 35-m-high Itkillik River bluff, 16 August 2007, 5:14 a.m.

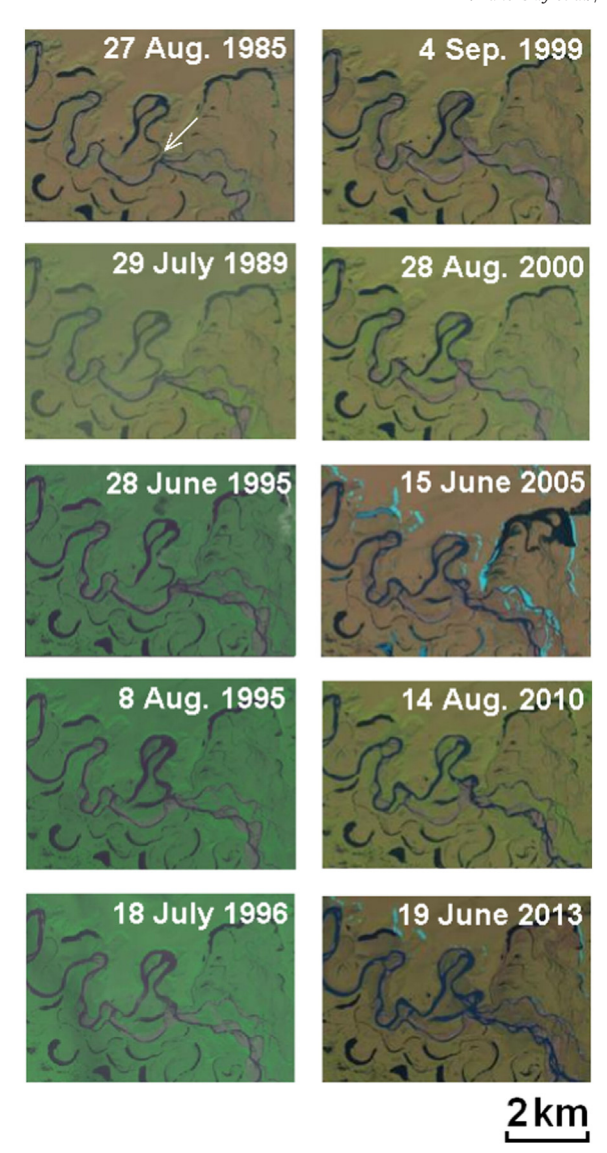


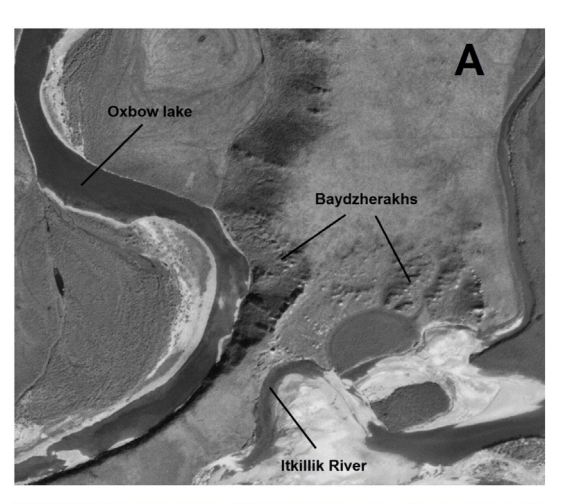
Fig. 7. Time-series of Landsat images of the study area (for location, see Fig. 1). Location of the bulkhead between the main river channel and the oxbow lake (site 1) is marked with white arrow in the 1985 image. The direction of flow is east to west.

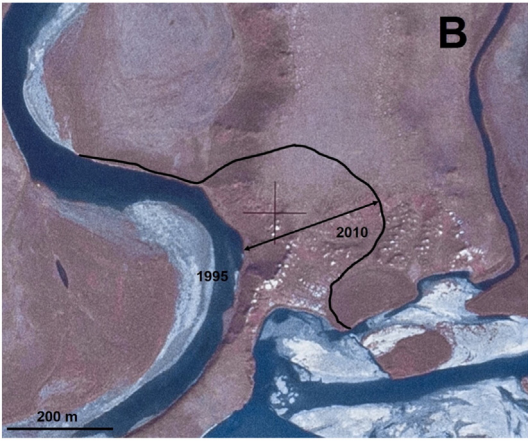
actively eroded central part of the bluff (~150 m long), the average retreat rate was 20.3 m/y and ranged from 16 to 24 m/y.

An analysis of aerial photographs (1948–1979) and satellite images (1974–2013) showed that the riverbank was relatively stable until 1995, when the Itkillik River abruptly changed its course (Fig. 7). Rapid degradation started when the bulkhead between the main river channel and an oxbow lake (central part of the pictures in Figs. 1B, 7) was destroyed by erosion. The oxbow lake was still separated from the main channel on 28 June 1995, but by 8 August 1995 the river water already filled the oxbow lake and adjacent area, and the river course changed dramatically (Fig. 7). It most likely happened in July 1995, and this event triggered extremely active thermal erosion of the previously stable bank of the former oxbow lake.

Long-term rates of erosion were estimated based on comparison of several available high-resolution images. On the aerial photograph of 4 August 1948 (Fig. 8A), the bank of the oxbow lake was stable; but baydzherakhs on the slope indicate that this bank had been actively eroded, presumably several decades before. Evidence of active riverbank erosion are visible at the floodplain bank and partially at the base of the yedoma slope on the other side of the bulkhead affected by the active river channel.

Comparison of the aerial photographs of 1948 and 1977 shows that during this period moderate riverbank erosion affected only the bulkhead from the side of the main river channel (Fig. 8A, B). The width of the bulkhead in 1948 was ~60 m (Fig. 8A), and it took 47 years for the bulkhead to be completely eroded in 1995. Thus, the rate of erosion was <1.3 m/y on average, but this process became more intense after 1989. We relate it to straightening of the main river channel upstream from the study site where several large meanders visible on images of 1948 to 1988 disappeared in 1989 (compare images of 1985 and 1989 in Fig. 7). Such straightening likely increased velocity of the stream and rate of erosion.





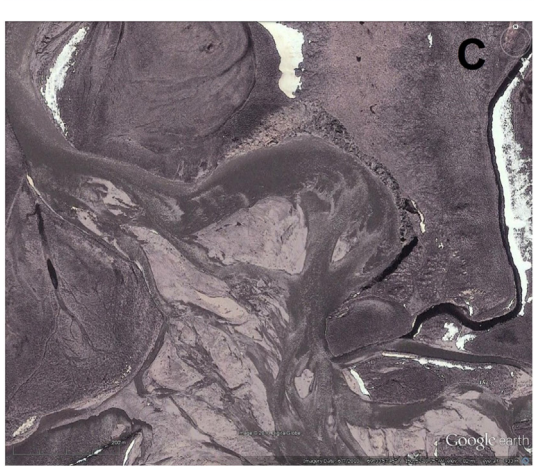
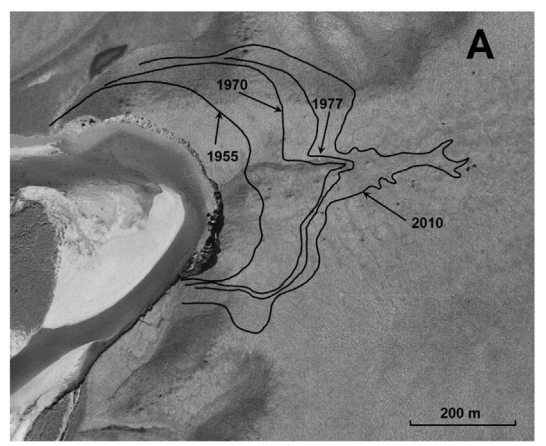


Fig. 8. Retreat of the Itkillik River yedoma bluff (site 1) from 1948 to 2010. (A) Aerial photograph, 4 August 1948. (B) Aerial photograph, 1 August 1977; the black line denotes the position of the river bank in June 2010 (note that the bluff remained generally stable from 1948 until July 1995). (C) Quickbird satellite image, 7 June 2010.

Table 3Retreat rates of yedoma bluffs degrading as a result of riverbank erosion.

Monitoring site	Height of the bluff, m	Observation period, years	Average retreat rate, m/y	Reference
Yana River, Mus-Khaya exposure, 190 km from the Laptev Sea	~40	36 (1953 to 1989)	6.5	Shur et al. (2002)
Indigirka River, Polyarnoye, 20 km from the East-Siberian Sea	~15	6 (1982 to 1988)	5.0	Shur et al. (2002)
Lena River delta	18	7 (2000 to 2006)	2.3	Grigoriev (2008)
Itkillik River (site 1), northern Alaska	34	4 (2007 to 2011)	2-24 ^a	This study
			(11.4 average)	
Itkillik River (site 1), northern Alaska	34	15 (1995 to 2010)	12-19 ^a	This study
Itkillik River (site 2), northern Alaska	~35	29 (1948 to 1977)	6-8 ^a	This study
Itkillik River (site 2), northern Alaska	~35	62 (1948 to 2010)	3-5 ^a	This study

^a Min-max, measured for different segments of the bluff.





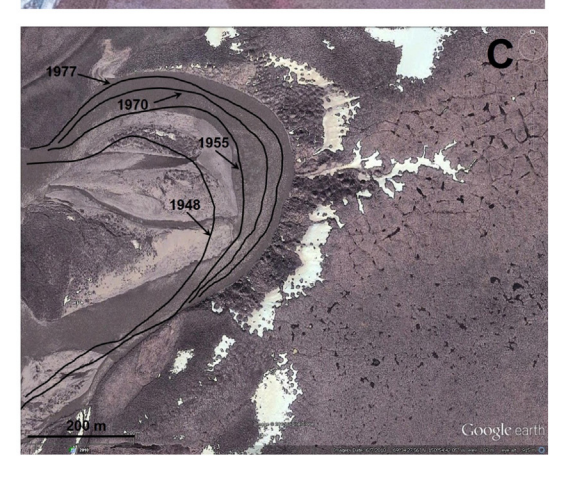


Fig. 9. Retreat of the Itkillik River yedoma bluff (site 2) from 1948 to 2010. (A) Aerial photograph of the site (4 August 1948); black lines denote position of the top of the retreating bluff in 1955, 1970, 1977, and 2010. (B) Aerial photograph of the site (1 August 1977). (C) Quickbird satellite image of the site (7 June 2010); black lines denote position of the river bank (base of the bluff) in 1948, 1955, 1970, and 1977.

The total retreat of the riverbank from 1977 to 2010, measured at the water level, varied from 180 to 280 m (Fig. 8B, C). Considering that active erosion started in July 1995, the average retreat rate for the most actively eroded part of the riverbank reached 19 m/y for the 15-year period.

Even in comparison with other yedoma sites in Eurasia and North America, such erosion rates over such a long time period are extremely high (Table 3). Higher rates of riverbank and coastal erosion of up to 55 m/y have been measured in Siberia for a short period, but the long-term rates at those sites in most cases did not exceed 10 m/y (Are, 1985). Such a high long-term rate of erosion requires numerous block falls and prevalence of thermal erosion over thermal denudation.

4.3.2. Rates of riverbank retreat at sites 2 and 3

We compared several available high-resolution images (1948 to 2010) of sites 2 and 3 previously described by Carter (1988) to evaluate rates of riverbank erosion and thermal denudation. No significant changes in riverbank position could be detected around site 3, but at site 2 (Fig. 1B) thermal erosion and thermal denudation had been active since 1948 (Fig. 9). In 1948, a sub-vertical yedoma bluff was separated from the river by a narrow lateral bar with several large blocks of frozen soil on its surface (substage 1c) (Fig. 9A). We interpret them as remnants of block falls, which probably occurred during a flooding event in the summer of 1948. The southern part of the bluff had been retreating mainly because of thermal denudation (probably, during several years before 1948) because only the upper part of the bluff was subvertical.

Long-term retreat rates measured on the top of bluffs with ice-rich permafrost are usually higher than the retreat rates measured at the base of the bluff (Are, 1985, 2012; Shur et al., 2002). Though thermal denudation is triggered by thermal erosion, in many cases it is independent of erosion at the base of the bluff and can continue for many years after complete termination of thermal erosion. This can be illustrated by the data obtained for site 2. Since 1948, the retreat rate of the base of the bluff was always lower than at the top (Fig. 9; Table 4), which means that the rate of thermal erosion was lower than the rate of thermal denudation (unlike site 1, where significant parts of the retreating bluff had been eroded by the river for many years). Total riverbank retreat from 1948 to 2010 measured at the base of the bluff varied at different segments of the bluff from 100 to 180 m, while total retreat measured on top varied from 180 to 320 m. The long-term rate of thermal denudation in 1948–2010 varied from 2.9 to 5.2 m/y, though its highest rates during 1948–1955 reached 14 m/y. These numbers are similar to the rates of thermal denudation measured at various yedoma sites in Siberia (Are, 1985; Shur et al., 2002) and Alaska (Swanson and Hill. 2010).

The rates of thermal denudation and thermal erosion at site 2 consistently decreased since the end of the 1970s (Table 4). Probably the decrease in height of the exposed bluff started in the 1980s because the exposed face of the northern part of the bluff in 1977 was still relatively high (Fig. 9B). This segment of the bluff showed a significant retreat from 1977 to 2010 (Fig. 9A). Carter (1988) described site 2 as a large, active thermokarst amphitheater with the exposed face of up to 15 m

Table 4Rates (min-max, m/y) of thermal erosion and thermal denudation of the Itkillik River yedoma bluff (site 2) from 1948 to 2010.

Years	1948-1955 (7 years)	1955–1970 (15 years)	1970–1977 (7 years)	1977–2010 (33 years)	1948–2010 (62 years)
Base of the bluff	5.7-12.9	0.8-3.4	1.2-4.2	0.2-0.8	1.6-2.9
(Thermal erosion and thermal denudation)					
Top of the bluff	8.6-14.3	3.9-7.0	1.2-9.0	0.4-2.5	2.9-5.2
(Thermal denudation and slumping)					

high and numerous baydzherakhs at the base of the active bluff (*substage 2b*). When we visited this site in August 2011, no frozen soils were exposed within the slope, and slope stabilization was in progress, though ice-wedge degradation, detected by poorly vegetated baydzherakhs and gully erosion, was still moderately active in places (*substages 3a* and *3b*).

4.4. Amount of eroded material

River erosion of yedoma bluffs results in transport of large volumes of water, mineral soil, and organic matter to the river from the retreating bank. To estimate the volumes of soil removed from the Itkillik River bluff (site 1) in 2007 to 2011, we divided the top surface of the entire 680-m-long exposure (the length is averaged between 2007 and 2011) into five segments with different modes of riverbank degradation during this period (Fig. 10). Characteristics of these segments presented in Table 5 were used for volume estimation with Eq. (3).

The total area of yedoma surface lost from 2007 to 2011 was $30,880 \text{ m}^2$. The area of the riverbank retreat during the same period at the water level was $20,800 \text{ m}^2$. The average retreat rate of the top edge of the bluff was 11.4 m/y. The average retreat rate of the riverbank at the water level was also significant and reached ~9.8 m/y. The highest retreat rates measured on top of the bluff and at the water level were similar and reached ~24 m/y.

The estimated total volume of ice and soil transported to the river from 2007 to 2011 was 731,520 m³, with an average annual loss of 182,880 m³/y. With average DD of 0.97 t/m³ and WIV of 61 vol.%, the mass of solid material lost from the bluff was estimated (Eq. (4)) to be 276,515 t, with an average annual loss of 69,179 t/y (Table 5). We estimated a total annual (2007 to 2011) organic carbon flux (Eqs. (1), (5); Table S2) based on an estimated volume of eroded material of 730,000 m³ and mean TOCD of 5 kg/m³ (adjusted for WIV of 61 vol.%), or more than 3500 t for the Itkillik River bluff, which is equal to 880 t of organic carbon per year. Generally, yedoma sequestered organic carbon was found to be of good quality for decomposition after thaw (Strauss et al., 2015).

Reimnitz et al. (1988) estimated that ~740,000 t of sediment were transported to the Beaufort Sea annually by the rivers between Drew Point and Prudhoe Bay, which includes Colville River and Kuparuk River basins. Such a comparison shows that erosion of the Itkillik River bluff represents a potential source for ~9% of this amount, though the fate of the sediments (including organic carbon) is unclear and only a small part of sediments is transported to the Arctic Ocean. Existing estimates show that about one-half of the sediment load of the Mackenzie River is accumulated within the Mackenzie Delta and cannot be delivered to the Beaufort Sea (Rachold et al., 2000).

Sediment input to the Itkillik River from the retreating bank can also be compared with that of the Omoloy River, which is located within the yedoma region of northern Yakutia. Zaikanov and Kanevskiy (1992a,b)

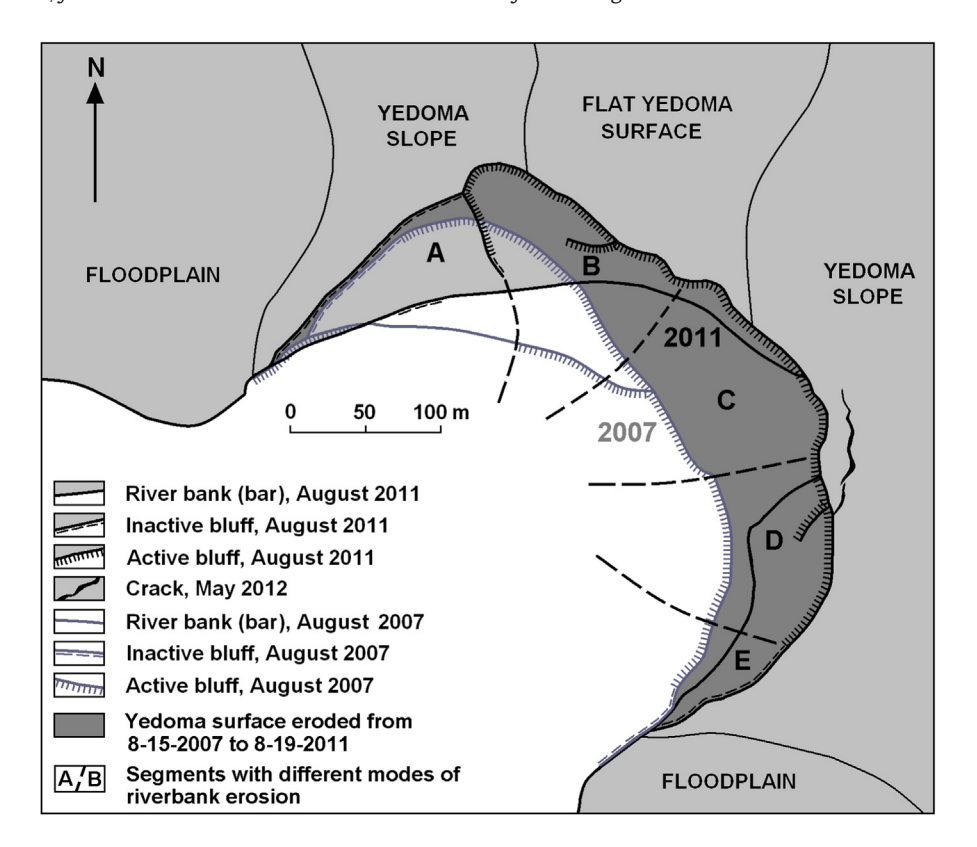


Fig. 10. Segments of the Itkillik River yedoma bluff (site 1) with different modes of riverbank erosion in 2007–2011. Characteristics of these segments are used for estimation of the amount of material transported to the river from the retreating bank (Table 5).

Table 5Characteristics of segments of the Itkillik River bluff (site 1) and estimation of volume of material transported to the river from the retreating bank from 2007 to 2011.

Segment	Stages of riverbank degradation 2007	Stages of riverbank degradation 2011	Segment length (m)	Average bluff height above river (m)	Height adjusted for calculations (m)	Average retreat in 2007 to 2011 (m/y)	Average retreat rate (m/y)	Area of degraded yedoma surface (m ²)	Total volume of frozen soils (m³)	Total weight of solids (t)	Organic carbon (t)
A	2b/3a/3b	3a/3b	170	15	5	9.4	2.4	1600	8000	3024	38
В	1/2b	2a/2b	140	30	30	44.6	11.2 ^a	6240	187,200	70,762	902
C	1	1/2a	150	33	33	81.1	20.3	12,160	401,280	151,684	1932
D	1	2b/3a	120	20	15	69.3	17.3	8320	124,800	47,174	600
E	1/(3a)	3a/3b	100	6	4	25.6	6.4	2560	10,240	3871	49
Total		_	680	_	_	_	_	30,880	731,520	276,515	3522
Average ^b	_	_	_	21.6	17.9	45.4	11.4	_	_		
Per year	_	_	-	-	-	11.4	11.4	7720	182,880	69,179	881

^a Retreat rate of 11.2 m/y was from thermal denudation of the upper part of the bluff (see Fig. 4B, section 2, profile B07-2–B11-2, *substage 2b*). Mutual action of thermal erosion and thermal denudation of the lower part of the bluff within this segment resulted in retreat rate of more than 18 m/y (see Fig. 4B, section 2, profile B07-1–B11-1", transformation from *substage 1a* to *substage 2b*).

found riverbank erosion, which affected the ice-rich floodplain deposits with large ice wedges and several small yedoma remnants, was responsible for more than 5,000,000 t of solids annually transported to the Omoloy River. With the total length of eroded banks (*stages 1* and 2) of 199 km within the studied stretch of the Omoloy River, the annual sediment input to the river reached more than 25,000 t/km, which is ~4 times less than that of the Itkillik River yedoma bluff.

5. Conclusions

Multiyear observations of riverbank erosion along a 35-m-high vertical yedoma bluff with extremely ice-rich permafrost revealed a sequence of geomorphic processes involved in erosion of bluff and exceptionally high rates of erosion. Thermal erosion and thermal denudation are two main processes defining riverbank erosion in the areas of ice-rich permafrost. Thermal erosion includes fast thawing of the frozen soil by running water at the base of the bluff with formation of deep thermoerosional niches. This results in the fall of large blocks of frozen ground, which finally disintegrate in water or on banks. Thermal denudation, a suite of processes specific to erosion in the areas of ice-rich permafrost, involves thawing of exposed frozen soil on the surface of the bluff because of solar radiation and convective heat exchange between the cold surface and the air and the flow of water and sediment down the bluff. Thermal denudation starts on the frozen face of a bluff exposed by thermal erosion and continues for years and even decades after the termination of thermal erosion. Thermal denudation during active thermal erosion reduces the total rate of erosion because it reduces the size of blocks of frozen soil above niches, and as a result, decreases stresses in frozen ground and ice above niches and therefore increases the duration of time periods between block-fall events. The process of riverbank erosion and stabilization include three main stages of riverbank evolution in a yedoma environment: (i) thermal erosion combined with thermal denudation; (ii) thermal denudation; and (iii) slope stabilization.

The average retreat rate for the whole 680-m-long bluff during 2007–2011 was estimated at 11.4 m/y, with some parts of the bluff eroding at 24 m/y. During the four years, 70,000 t of solids per year, including ~880 t of organic carbon, were transported to the river from the retreating bank. From 1995 to 2010, the average retreat rate for the most actively eroded part of the riverbank was 19 m/y. This rate is higher than any other long-term rates of riverbank erosion previously reported for permafrost regions of Eurasia and North America.

Acknowledgments

Study was mainly supported by the National Science Foundation (NSF) grant ARC 1023623. J.S. acknowledges the German Federal Ministry of Education and Research (grant 01DM12011), the German National Academic Foundation (Studienstiftung des Deutschen Volkes),

ERC grant #338335, and the Initiative and Networking Fund of the Helmholtz Assoc. (#ERC-0013) for financial support. D.F. acknowledges the National Sciences and Engineering Council of Canada (1072150) for financial support. We greatly appreciate CH2M HILL Polar Services for the logistical support. We thank Kevin Bjella, Amy Breen, Tripp Collier, Hugh French, and Cody Johnson for their participation in the field work at the study site. We would like to thank Editor Dr. Richard Marston and three anonymous reviewers whose valuable comments and suggestions helped to improve the manuscript.

Appendix A. Supplementary data

Supplementary data associated with this article can be found in the online version, at http://dx.doi.org/10.1016/j.geomorph.2015.10.023. These data include the Google maps of the most important areas described in this article.

References

Are, F.E., 1968. Razvitie reliefa termoabrazionnykh beregov [Terrain development of thermo-abrasional shores] Izvestiya (Transactions) of the USSR Academy of Sciences. Geography 1, 92–100 (in Russian).

Are, F.E., 1980. Termoabraziya morskikh beregov (Thermal abrasion of seashores). Nauka Press, Moscow (157 pp., in Russian).

Are, F.E., 1985. Osnovy prognoza termoabrazii beregov (Fundamentals of forecast of thermal abrasion of shores). Nauka Press, Moscow (173 pp., in Russian).

Are, F.E., 1988. Thermal abrasion of sea coasts (part 2). Polar Geogr. Geol 12 (2), 87–157. http://dx.doi.org/10.1080/10889378809377352.

Are, F.E., 2012. Razrushenie beregov arkticheskikh primorskikh nizmennostey (Coastal erosion of the Arctic lowlands). Academic Publishing House "Geo", Novosibirsk (291 pp., in Russian).

Bray, M.T., French, H.M., Shur, Y., 2006. Further cryostratigraphic observations in the CRREL permafrost tunnel, Fox, Alaska. Permafr. Periglac. Process. 17 (3), 233–243.

Brewer, M.C., Carter, L.D., Glenn, R., 1993. Sudden drainage of a thaw lake on the Alaskan Arctic Coastal Plain. Proceedings of the Sixth International Conference on Permafrost, July 5–9, Beijing, China. South China University of Technology Press, pp. 48–53.

Brice, J.C., 1973. Measurement of lateral erosion at proposed river crossing sites of the Alaska pipeline. U.S. Geological Survey Open-File Report 73–31 (39 pp.).

Carter, L.D., 1988. Loess and deep thermokarst basins in Arctic Alaska. Proceedings of the Fifth International Conference on Permafrost. Tapir Publishers, Trondheim, Norway, pp. 706–711.

Costard, F., Dupeyrat, L., Gautier, E., Carey-Gailhardis, E., 2003. Fluvial thermal erosion investigations along a rapidly eroding river bank: application to the Lena River (Central Siberia). Fluvial Earth Surf. Process. Landf. 28, 1349–1359.

Couture, N.J., Hoque, M.A., Pollard, W.H., 2008. Modelling the erosion of ice-rich deposits along the Yukon Coastal Plain. In: Kane, D.L., Hinkel, K.M. (Eds.), Proceedings of the Ninth International Conference on Permafrost, June 29–July 3, 2008 vol. 1. Institute of Northern Engineering, University of Alaska Fairbanks, Fairbanks, Alaska, pp. 303–308.

Czudek, T., Demek, J., 1973. Thermokarst in Siberia and its influence on the development of lowland relief. Ouat. Res. 1, 103–120.

van Everdingen, R.O. (Ed.), 1998. Multi-Language Glossary of Permafrost and Related Ground-Ice Terms. International Permafrost Association, University of Calgary.

Ferreira T., Rasband W.S., 2012. ImageJ user guide — IJ 1.46. imagej.nih.gov/ij/docs/guide/. http://rsbweb.nih.gov/ij/docs/guide/user-guide.pdf, (accessed 2 October 2012)

Fortier, D., Allard, M., 2004. Late Holocene syngenetic ice-wedge polygons development, Bylot Island, Canadian Arctic Archipelago. Can. J. Earth Sci. 41, 997–1012.

^b Weighted with the length of segments.

- Fortier, D., Allard, M., Shur, Y., 2007. Observation of rapid drainage system development by thermal erosion of ice wedges on Bylot Island, Canadian Arctic Archipelago. Permafr. Periglac. Process. 18 (3), 229–243.
- Fraser, T.A., Burn, C.R., 1997. On the nature and origin of "muck" deposits in the Klondike area, Yukon Territory, Can. J. Earth Sci. 34, 1333–1344.
- French, H.M., 2007. The Periglacial Environment. 3rd ed. John Wiley and Sons Ltd., Chichester, UK (458 pp.).
- Fritz, M., Opel, T., Tanski, G., Herzschuh, U., Meyer, H., Eulenburg, A., Lantuit, H., 2015. Dissolved organic carbon (DOC) in Arctic ground ice. Cryosphere 9, 737–752. http://dx.doi.org/10.5194/tc-9-737-2015.
- Froese, D.G., Zazula, G.D., Westgate, J.A., Preece, S.J., Sanborn, P.T., Reyes, A.V., Pearce, N.J.G., 2009. The Klondike goldfields and Pleistocene environments of Beringia. GSA Today 19 (8), 4–10. http://dx.doi.org/10.1130/GSATG54A.1.
- Godin, E., Fortier, D., 2012. Fine-scale spatio-temporal monitoring of multiple thermoerosion gullies development on Bylot Island, Eastern Canadian Archipelago. Proceedings of the 10th International Conference on Permafrost, June 25–29, Salekhard, Russia vol. 1, pp. 125–130.
- Gordeev, V.V., 2006. Fluvial sediment flux to the Arctic Ocean. Geomorphology 80, 94–104.
- Grechishchev, S.E., Shur, Y. (Eds.), 1990. Metodicheskie rekomendatsii po uchyotu sostava i strukturno-teksturnogo stroeniya myorzlykh porod pri prognoze razvitiya kriogennykh fiziko-geologicheskikh protsessov. (Implementation of composition and structure of frozen ground in prediction of permafrost related geological hazards (manual)). Ministry of Geology of USSR, Moscow (79 pp., in Russian).
- Grigoriev, M.N., 2008. Kriomorphogenez i litodinamika pribrezhno-shelfovoy zony morey Vostochnoy Sibiri (Cryomorphogenesis and lithodynamics of coastal-shelf zone of the seas of East Siberia). Avtoreferat dissertatsii na soiskanie uchenoy stepeni doktora geograficheskikh nauk. (Synopsis of the Doctor of Science thesis). Permafrost Institute SB RAS, Yakutsk (40 pp., in Russian).
- Grigoriev, M., Rachold, V., 2003. The degradation of coastal permafrost and the organic carbon balance of the Laptev and East Siberian Seas. Proceedings of the 8th International conference on permafrost, 21–25 July 2003, Zurich, Switzerland vol. 1, pp. 319–324.
- Grosse, G., Harden, J., Turetsky, M., McGuire, D.A., Camill, P., Tarnocai, C., Frolking, C., Schuur, E.A.G., Jorgenson, T., Marchenko, S., Romanovsky, V., Wickland, K.P., French, N., Waldrop, M., Bourgeau-Chavez, L., Striegl, R.G., 2011. Vulnerability of highlatitude soil organic carbon in North America to disturbance. J. Geophys. Res. 116, G00K06. http://dx.doi.org/10.1029/2010JG001507.
- Günther, F., Overduin, P.P., Sandakov, A.V., Grosse, G., Grigoriev, M.N., 2013. Short- and long-term thermo-erosion of ice-rich permafrost coasts in the Laptev Sea region. Biogeosciences 10, 4297–4318. http://dx.doi.org/10.5194/bg-10-4297-2013.
- Hamilton, T.D., 1994. Late Cenozoic glaciation of Alaska. In: Plafker, G., Berg, H.C. (Eds.), The Geology of Alaska: The Geology of North America vol. G-1. Geological Society of America, Boulder, Colorado, pp. 813–844.
- Hamilton, T.D., Craig, J.L., Sellmann, P.V., 1988. The Fox permafrost tunnel: a late Quaternary geologic record in central Alaska. Geol. Soc. Am. Bull. 100, 948–969.
- Hinkel, K.M., Sheng, Y., Lenters, J.D., Lyons, E.A., Beck, R.A., Eisner, W.R., Wang, J., 2012. Thermokarst lakes on the Arctic Coastal Plain of Alaska: geomorphic controls on bathymetry. Permafr. Periglac. Process. 23, 218–230. http://dx.doi.org/10.1002/ppp.1744.
- Hopkins, D.M., 1963. Geology of the Imuruk Lake area, Seward Peninsula, Alaska. U.S. Geol. Surv. Bull. 1141-c (101 pp.).
- Hoque, M.A., Pollard, W.H., 2009. Arctic coastal retreat through block failure. Can. Geotech. J. 46, 1103–1115. http://dx.doi.org/10.1139/T09-058.
- Ivanov, M.S., 1984. Kriogennoe stroenie chetvertichnykh otlozheniy Leno-Aldanskoy vpadiny (Cryogenic structure of the Quaternary deposits of Lena-Aldan lowland). Nauka Press, Novosibirsk (126 pp., In Russian).
- Jensen, B.J.L., Reyes, A.V., Froese, D.G., Stone, D.B., 2013. The Palisades is a key reference site for the middle Pleistocene of eastern Beringia: new evidence from paleomagnetics and regional tephrostratigraphy. Quat. Sci. Rev. 63, 91–108.
- Jones, B.M., Arp, C.D., Jorgenson, M.T., Hinkel, K.M., Schmutz, J.A., Flint, P.L., 2009. Increase in the rate and uniformity of coastline erosion in Arctic Alaska. Geophys. Res. Lett. 36, L03503. http://dx.doi.org/10.1029/2008GL036205.
- Jones, B.M., Grosse, G., Arp, C.D., Jones, M.C., Walter Anthony, K.M., Romanovsky, V.E., 2011. Modern thermokarst lake dynamics in the continuous permafrost zone, northern Seward Peninsula, Alaska. J. Geophys. Res. 116, G00M03. http://dx.doi.org/10. 1029/2011|G001666.
- Jorgenson, M.T. (Ed.), 2011. Coastal region of northern Alaska. Guidebook to permafrost and related features. Alaska Division of Geological & Geophysical Surveys, Guidebook 10 (188 pp.).
- Jorgenson, M.T., Brown, J., 2005. Classification of the Alaskan Beaufort Sea Coast and estimation of carbon and sediment inputs from coastal erosion. Geo-Mar. Lett. 25, 69–80.
- Jorgenson, M.T., Kanevskiy, M., Shur, Y., Grunblatt, J., Ping, C.L., Michaelson, G., 2014. Permafrost database development, characterization, and mapping for northern Alaska. Report for Arctic Landscape Conservation Cooperative by Alaska Ecoscience and University of Alaska Fairbanks (45 pp., http://www.gina.alaska.edu/projects/permafrost-database-and-maps-for-northern-alaska).
- Jorgenson, T., Yoshikawa, K., Kanevskiy, M., Shur, Y., Romanovsky, V., Marchenko, S., Grosse, G., Brown, J., Jones, B., 2008. Permafrost characteristics of Alaska. In: Kane, D.L., Hinkel, K.M. (Eds.), Proceedings of the Ninth International Conference on Permafrost, Extended Abstracts. June 29-July 3, 2008, Fairbanks, Alaska. Institute of Northern Engineering, University of Alaska Fairbanks, pp. 121–122.
- Kane, D.L., Youcha, E.K., Stuefer, S.L., Myerchin-Tape, G., Lamb, E., Homan, J.W., Gieck, R.E., Schnabel, W.E., Toniolo, H., 2014. Hydrology and meteorology of the central Alaskan Arctic: data collection and analysis. Final Report. University of Alaska Fairbanks, Water and Environmental Research Center, Report INE/WERC 14.05, Fairbanks, Alaska (169 pp.).

- Kanevskiy, M., Shur, Y., Jorgenson, M.T., Ping, C.-L., Michaelson, G.J., Fortier, D., Stephani, E., Dillon, M., Tumskoy, V., 2013a. Ground ice in the upper permafrost of the Beaufort Sea Coast of Alaska. Cold Reg. Sci. Technol. 85, 56–70. http://dx.doi.org/10.1016/j.coldregions.2012.08.002.
- Kanevskiy, M.Z., Shur, Y., Krzewinski, T., Dillon, M., 2013b. Structure and properties of icerich permafrost near Anchorage, Alaska. Cold Reg. Sci. Technol. 93, 1–11. http://dx.doi.org/10.1016/j.coldregions.2013.05.001.
- Kanevskiy, M., Fortier, D., Shur, Y., Bray, M., Jorgenson, T., 2008. Detailed cryostratigraphic studies of syngenetic permafrost in the winze of the CRREL permafrost tunnel, Fox, Alaska. In: Kane, D.L., Hinkel, K.M. (Eds.), Proceedings of the Ninth International Conference on Permafrost, June 29-July 3, 2008 vol. 1. Institute of Northern Engineering, University of Alaska Fairbanks, Fairbanks, Alaska, pp. 889–894.
- Kanevskiy, M., Jorgenson, M.T., Shur, Y., O'Donnell, J.A., Harden, J.W., Zhuang, Q., Fortier, D., 2014. Cryostratigraphy and permafrost evolution in lacustrine lowlands of west-central Alaska. Permafr. Periglac. Process. 25 (1), 14–34. http://dx.doi.org/10.1002/ppp.1800.
- Kanevskiy, M., Shur, Y., Connor, B., Dillon, M., Stephani, E., O'Donnell, J., 2012. Study of the ice-rich syngenetic permafrost for road design (Interior Alaska). In: Hinkel, K.M. (Ed.)Proceedings of the Tenth International Conference on Permafrost, June 25–29, 2012, Salekhard, Russia. International Contributions vol. 1. The Northern Publisher, Salekhard, Russia, pp. 191–196.
- Kanevskiy, M., Shur, Y., Fortier, D., Jorgenson, M.T., Stephani, E., 2011. Cryostratigraphy of late Pleistocene syngenetic permafrost (yedoma) in northern Alaska, Itkillik River exposure. Quat. Res. 75, 584–596.
- Kotler, E., Burn, C.R., 2000. Cryostratigraphy of the Klondike "muck" deposits, westcentral Yukon Territory. Can. J. Earth Sci. 37, 849–861.
- Lantuit, H., Overduin, P.P., Couture, N., Ødegård, R.S., 2008. Sensitivity of coastal erosion to ground ice contents: an Arctic-wide study based on the ACD classification of Arctic coasts. In: Kane, D.L., Hinkel, K.M. (Eds.), Ninth International Conference on Permafrost vol. 1. Institute of Northern Engineering, University of Alaska Fairbanks, pp. 1025–1029.
- Lantuit, H., Overduin, P.P., Couture, N., Wetterich, S., Are, F., Atkinson, D., Brown, J., Cherkashov, G., Drozdov, D., Forbes, D., Graves-Gaylord, A., Grigoriev, M., Hubberten, H.W., Jordan, J., Jorgenson, T., Ødegård, R.S., Ogorodov, S., Pollard, W., Rachold, V., Sedenko, S., Solomon, S., Steenhuisen, F., Streletskaya, I., Vasiliev, A., 2012. The Arctic coastal dynamics database: a new classification scheme and statistics on Arctic permafrost coastlines. Estuar. Coasts 35, 383–400.
- Lantuit, H., Overduin, P.P., Wetterich, S., 2013. Recent progress regarding permafrost coasts. Permafr. Periglac. Process. 24, 120–130. http://dx.doi.org/10.1002/ppp.1777.
- Lawson, D.E., 1983. Erosion of perennially frozen streambanks. CRREL Report 83-29 (22 pp.).
- Leffingwell, E.d.K., 1915. Ground-ice wedges, the dominant form of ground-ice on the north coast of Alaska. J. Geol. 23, 635–654.
- Leffingwell, E.d.K., 1919. The Canning River region, Northern Alaska. U.S. Geological Survey professional paper 109. United States Government Printing Office, Washington (251 pp.)
- Livingstone, D.A., Bryan Jr., K., Leahy, R.G., 1958. Effects of an Arctic environment on the origin and development of freshwater lakes. Limnol. Oceanogr. 3, 192–214.
- Miles, M., 1976. An investigation on riverbank and coastal erosion, Banks Island, District of Franklin. Geological Survey of Canada, Report of Activities Part A, Paper 76-1A, pp. 195–200.
- Murton, J.B., Goslar, T., Edwards, M.E., Bateman, M.D., Danilov, P.P., Savvinov, G.N., Gubin, S.V., Ghaleb, B., Haile, J., Kanevskiy, M., Lozhkin, A.V., Lupachev, A.V., Murton, D.K., Shur, Y., Tikhonov, A., Vasil'chuk, A.C., Vasil'chuk, Y.K., Wolfe, S.A., 2015. Palaeoenvironmental interpretation of yedoma silt (ice complex) deposition as cold-climate loess, Duvanny Yar, Northeast Siberia. Permafr. Periglac. Process. 26, 208–288.
- Nossov, D.R., Jorgenson, M.T., Kielland, K., Kanevskiy, M.Z., 2013. Edaphic and microclimatic controls over permafrost response to fire in interior Alaska. Environ. Res. Lett. 8 (3), 035013. http://dx.doi.org/10.1088/1748-9326/8/3/035013 (12 pp.).
- Outhet, D.N., 1974. Bank erosion in the southern Mackenzie River Delta (M.S. Thesis) University of Alberta, Edmonton, Alberta (89 pp.).
- Péwé, T.L., 1975. Quaternary geology of Alaska. U.S. Geological Survey professional paper 835. United States Government Printing Office, Washington (145 pp.).
- Ping, C.-L., Michaelson, G.J., Guo, L., Jorgenson, M.T., Kanevskiy, M., Shur, Y., Dou, F., Liang, J., 2011. Soil carbon and material fluxes across the eroding Alaska Beaufort Sea coastline. J. Geophys. Res. Biogeosci. 116, G02004. http://dx.doi.org/10.1029/2010JG001588.
- Rachold, V., Grigoriev, M.N., Are, F.E., Solomon, S., Reimnitz, E., Kassens, H., Antonow, M., 2000. Coastal erosion vs riverine sediment discharge in the Arctic shelf seas. Int. J. Earth Sci. 89 (3), 450–460.
- Reimnitz, E., Graves, S.M., Barnes, P.W., 1988. Beaufort Sea coastal erosion, sediment flux, shoreline evolution, and the erosional shelf profile. U.S. Geological Survey Miscellaneous Investigations Series, Map I-1182-G.
- Romanovskii, N.N., Hubberten, H.-W., Gavrilov, A.V., Tumskoy, V.E., Kholodov, A.L., 2004. Permafrost of the east Siberian Arctic shelf and coastal lowlands. Quat. Sci. Rev. 23, 1350, 1360
- Schirrmeister, L., Froese, D., Tumskoy, V., Grosse, G., Wetterich, S., 2013. Yedoma: Late Pleistocene ice-rich syngenetic permafrost of beringia. Encyclopedia of Quaternary Science, Second edition, pp. 542–552.
- Schuur, E.A.G., McGuire, A.D., Schädel, C., Grosse, G., Harden, J.W., Hayes, D.J., Hugelius, G., Koven, C.D., Kuhry, P., Lawrence, D.M., Natali, S.M., Olefeldt, D., Romanovsky, V.E., Schaefer, K., Turetsky, M.R., Treat, C.C., Vonk, J.E., 2015. Climate change and the permafrost carbon feedback. Nature 520, 171–179. http://dx.doi.org/10.1038/nature14338.
- Scott, K.M., 1978. Effects of permafrost on stream channel behavior in Arctic Alaska. U.S. Geological Survey professional paper 1068. United States Government Printing Office, Washington (19 pp.).

- Sher, A.V., 1997. A brief overview of the late Cenozoic history of the western Beringian lowlands. In: Edwards, M.E., Sher, A.V., Guthrie, R.D. (Eds.), Terrestrial paleoenvironmental studies in BeringiaProceedings of a joint Russian-American Workshop. Fairbanks, Alaska, June 1991. Alaska Quaternary Center, pp. 3–7.
- Shur, Y.L., 1988. Verkhniy gorizont tolshchi myorzlykh porod i termokarst (Upper horizon of permafrost and thermokarst). Nauka Press, Novosibirsk (210 pp., in Russian).
- Shur, Y., Osterkamp, T., 2007. Thermokarst. Report INE 06.11. University of Alaska Fairbanks, Institute of Northern Engineering, Fairbanks, Alaska (50 pp.).
- Shur, Y.L., Vasiliev, A.A., 1978. Opyt izucheniya baydzharakhov na severe Yakutii (Study of baydzherakhs in Northern Yakutia). In: Grechishchev, S.E., Chistotinov, L.V., Shur, Y.L. (Eds.), Kriogennie protsessy. (Cryogenic Processes). Nauka Press, Moscow, pp. 220–233.
- Shur, Y., French, H.M., Bray, M.T., Anderson, D.A., 2004. Syngenetic permafrost growth: cryostratigraphic observations from the CRREL Tunnel near Fairbanks, Alaska. Permafr. Periglac. Process. 15 (4), 339–347.
- Shur, Y., Kanevskiy, M., Jorgenson, T., Dillon, M., Stephani, E., Bray, M., 2012. Permafrost degradation and thaw settlement under lakes in yedoma environment. In: Hinkel, K.M. (Ed.), Proceedings of the Tenth International Conference on PermafrostInternational Contributions, June 25–29, 2012, Salekhard, Russia vol. 1. The Northern Publisher, Salekhard, Russia, pp. 383–388.
- Shur, Y., Vasiliev, A., Kanevskiy, M., Maksimov, V., Pokrovsky, S., Zaikanov, V., 2002. Shore erosion in Russian Arctic. Cold Region Impacts on Transportation and Infrastructure. ASCE, pp. 736–747.
- Shur, Y.L., Vasiliev, A.A., Veisman, L.I., Zaikanov, V.G., Maksimov, V.V., Petrukhin, N.P., 1984. Novye rezul'taty nablyudeniy za razrusheniem beregov v kriolitozone (New data of monitoring of shore erosion in permafrost region). In: Are, F.E. (Ed.), Beregovye protsessy v kriolitozone. (Shore processes in permafrost region). Nauka Press, Novosibirsk, pp. 12–19.
- Solomon, S.M., 2005. Spatial and temporal variability of shoreline change in the Beaufort-Mackenzie region, Northwest Territories, Canada. Geo-Mar. Lett. 25, 127–137.
- Soloviev, P.A., 1962. Alasniy relief Tsentral'noy Yakutii I ego proiskhozhdenie (Alas relief of Central Yakutia and its origin). In: Grave, N.A. (Ed.), Mnogoletnemyorzlye porody i soputstvuyushchie im yavleniya na territirii Yakutskoy ASSR [Permafrost and related features in Central Yakutia]. The Academy of Sciences of the USSR Press, Moscow, pp. 38–54 (in Russian).
- Stephani, E., Fortier, D., Shur, Y., Fortier, R., Doré, G., 2014. A geosystems approach to permafrost investigations for engineering applications, an example from a road stabilization experiment, Beaver Creek, Yukon, Canada. Cold Reg. Sci. Technol. 100, 20–35. http://dx.doi.org/10.1016/j.coldregions.2013.12.006.
- Strauss, J., Schirrmeister, L., Wetterich, S., Borchers, A., Davydov, S.P., 2012a. Grain-size properties and organic-carbon stock of yedoma ice complex permafrost from the Kolyma lowland, northeastern Siberia. Glob. Biogeochem. Cycles 26, GB3003. http://dx.doi.org/10.1029/2011GB004104.
- Strauss, J., Shur, Y., Kanevskiy, M., Fortier, D., Bjella, K., Breen, A., Johnson, C., 2012b. Expedition Alaskan North Slope/Itkillik 2012. In: Strauss, J., Ulrich, M., Buchhorn, M. (Eds.), Expeditions to permafrost 2012: Alaskan North Slope/Itkillik, Thermokarst in Central Yakutia, and EyeSight-NAAT-AlaskaReports on Polar and Marine Research, Bremerhaven 655. Alfred Wegener Institute for Polar and Marine Research, pp. 3–28.
- Strauss, J., Schirrmeister, L., Grosse, G., Wetterich, S., Ulrich, M., Herzschuh, U., Hubberten, H.-W., 2013. The deep permafrost carbon pool of the Yedoma region in Siberia and Alaska. Geophys. Res. Lett. 40, 6165–6170. http://dx.doi.org/10.1002/2013GL058088.

- Strauss, J., Schirrmeister, L., Mangelsdorf, K., Eichhorn, L., Wetterich, S., Herzschuh, U., 2015. Organic-matter quality of deep permafrost carbon a study from Arctic Siberia. Biogeosciences 12 (7), 2227–2245. http://dx.doi.org/10.5194/bg-12-2227-2015.
- Swanson, D.K., Hill, K., 2010. Monitoring of retrogressive thaw slumps in the Arctic Network, 2010 baseline data: three-dimensional modeling with small-format aerial photographs. Natural Resource Data Series NPS/ARCN/NRDS—2010/123. National Park Service, Fort Collins, Colorado.
- Tomirdiaro, S.V., 1980. Lyossovo-ledovaya formatsiya Vostochnoy Sibiri v pozdnem pleistotsene i golotsene (Loess-ice formation of Eastern Siberia in the Late Pleistocene and Holocene). Nauka, Moscow (184 pp., in Russian).
- U.S. Geological Survey, 1971. Topographic maps of Alaska 1:63,360 Available at: http://www.gina.alaska.edu/data.
- U.S. Geological Survey, 2014. Aerial photographs and satellite images. Available at: http://earthexplorer.usgs.gov/.
- Ulrich, M., Grosse, G., Strauss, J., Schirrmeister, L., 2014. Quantifying wedge-ice volumes in yedoma and thermokarst basin deposits. Permafr. Periglac. Process. 25 (3), 151–161.
- Vasiliev, A.A., 2003. Permafrost controls of coastal dynamics at the Marre-Sale key site, western Yamal Peninsula, Siberia. Proceedings, Eighth International Conference on Permafrost, 21–25 July 2003, Zurich 2. A.A. Balkema Publishers, pp. 1173–1178.
- Vasiliev, A.A., Pokrovsky, S.I., Shur, Y.L., 2001. Dinamika termoabrazionnykh beregov Zapadnogo Yamala (Dynamics of the coastal thermoerosion of West Yamal). Kriosfera Zemli (Earth Cryosphere) V (1), 44–52 (in Russian).
- Walker, H.J., 1983. Guidebook to permafrost and related features of the Colville River delta, Alaska. Guidebook 2, Fourth International Conference on Permafrost, July 18–22, 1983. University of Alaska Fairbanks, USA (34 pp.).
- Walker, H.J., Arnborg, L., 1966. Permafrost and ice-wedge effect on riverbank erosion. Proceedings of the International Conference on Permafrost, Lafayette, Indiana, 11–15 November 1963. National Academy of Sciences—National Research Council, Washington, D.C., Publication 1287, pp. 164–171.
- Walker, H.J., Jorgenson, M.T., 2011. Tour of the Colville River delta. In: Jorgenson, M.T. (Ed.), 2011. Coastal region of northern Alaska. Guidebook to permafrost and related features. Alaska Division of Geological & Geophysical surveys, Guidebook 10, Part 4, pp. 85–135.
- Walker, J., Arnborg, L., Peippo, J., 1987. Riverbank erosion in the Colville Delta, Alaska. Geogr. Ann. Ser. A Phys. Geogr. 69 (1), 61–70.
- Williams, J.R., 1952. Effect of wind-generated waves on migration of the Yukon River in the Yukon Flats, Alaska. Science 115 (2993), 519–520.
- Williams, J.R., 1962. Geologic reconnaissance of the Yukon Flats district, Alaska. U.S. Geological Survey Bulletin 1111-H. United States Government Printing Office, Washington, DC, pp. 290–311.
- Zaikanov, V., Kanevskiy, M., 1992a. Prichiny zagryazneniya Yany i Omoloya [The causes of contamination of the Yana and Omoloy Rivers]. Priroda [Nature] 9, 90–94 (in Russian)
- Zaikanov, V., Kanevskiy, M., 1992b. Beregovie protsessy v dolinakh krupnikh rek Severnoy Yakutii (The riverbank erosion in the valleys of large rivers in Northern Yakutia). In: Grechishchev, S., Vasiliev, A., Sheshin, Y. (Eds.), Metody izucheniya kriogennykh fiziko-geologicheskikh protsessov. (Methods of Study of Cryogenic Processes). VSEGINGEO, Moscow, pp. 16–29 (in Russian).
- Zhang, T., Osterkamp, T.E., Stamnes, K., 1996. Some characteristics of the climate in northern Alaska, U.S.A. Arct. Alp. Res. 28 (4), 509–518.